Solid Earth, 11, 1823–1847, 2020
https://doi.org/10.5194/se-11-1823-2020

Solid Earth Open Access EGU

Long-wavelength late-Miocene thrusting in the north Alpine foreland: implications for late orogenic processes

Samuel Mock[1], **Christoph von Hagke**[2,3], **Fritz Schlunegger**[1], **István Dunkl**[4], **and Marco Herwegh**[1]

[1]Institute of Geological Sciences, University of Bern, Baltzerstrasse 1+3, 3012 Bern, Switzerland
[2]Institute of Geology and Palaeontology, RWTH Aachen University, Wüllnerstrasse 2, 52056 Aachen, Germany
[3]Department of Geography and Geology, University of Salzburg, Hellbrunnerstrasse 34, 5020 Salzburg, Austria
[4]Geoscience Center, Sedimentology and Environmental Geology, University of Göttingen, Goldschmidtstrasse 3, 37077 Göttingen, Germany

Correspondence: Samuel Mock (samuel.mock@geo.unibe.ch)

Received: 17 October 2019 – Discussion started: 27 November 2019
Revised: 24 August 2020 – Accepted: 25 August 2020 – Published: 13 October 2020

Abstract. In this paper, we present new exhumation ages for the imbricated proximal molasse, i.e. Subalpine Molasse, of the northern Central Alps. Based on apatite (U−Th−Sm)/He thermochronometry, we constrain thrust-driven exhumation in the Subalpine Molasse between 12 and 4 Ma. This occurs synchronously to the main deformation in the adjacent Jura fold-and-thrust belt farther north and to the late stage of thrust-related exhumation of the basement massifs (i.e. external crystalline massifs) in the hinterland. Our results agree with other findings along the north Alpine foreland. While site-specific variations in the mechanical stratigraphy of the molasse deposits influence the pattern of thrusting at the local scale, we observe that late-Miocene thrusting is a long-wavelength feature occurring along the north Alpine foreland roughly between Lake Geneva and Salzburg. The extent of this thrusting signal as well as the timing suggests that late-Miocene thrusting in the north Alpine foreland coincides with the geometries and dynamics of the attached Central Alpine slab at depth. Interestingly, this implies that the slab geometry at depth does not coincide with the boundary between the Eastern and Central Alps as observed in the surface geology. Using this observation, we propose that thrusting in the Subalpine Molasse and consequently also the late stage of thrust-related exhumation of the external crystalline massifs, as well as the main deformation in the Jura fold-and-thrust belt are at least partly linked to changes in slab dynamics.

1 Introduction

Deep crustal processes and slab dynamics have been considered to influence the evolution of mountain belts (e.g. Davies and von Blanckenburg, 1995; Molnar et al., 1993; Oncken et al., 2006). However, these deep-seated signals may be masked by tectonic forcing at upper-crustal levels and by enhanced surface erosion related to climate change (e.g. Champagnac et al., 2007; Chemenda et al., 2000; Ganti et al., 2016; Whipple, 2009; Willett et al., 2006). In near-surface crustal domains, it is thus challenging to isolate the exhumation signal related to slab dynamics. In this context, foreland basins offer suitable archives as they potentially bear information that allows us to resolve the influence of deep-seated processes on mountain building. This is the case because these basins not only record signals that are related to surface dynamics such as changes in sediment fluxes and eustacy (e.g. Pippèrr and Reichenbacher, 2017; Sinclair and Allen, 1992), but they also preserve information on the tectonic processes at the crustal and possibly mantle scales that operate on long timescales and at long spatial wavelengths (e.g. DeCelles and Giles, 1996; Garefalakis and Schlunegger, 2018; Leary et al., 2016). The north Alpine foreland basin, or Molasse Basin, is particularly suited to constrain the geodynamic evolution of the collisional Alpine orogen because the history of this sedimentary trough has been well established through numerous magneto- and tectonostratigraphic (e.g. Burkhard and Sommaruga, 1998; Ganss and Schmidt-Thomé, 1953; Homewood et al., 1986; Kempf et al., 1999;

Pfiffner, 1986; Schlunegger et al., 1996; Sinclair et al., 1991), seismic (Hinsch, 2013; Mock and Herwegh, 2017; Ortner et al., 2015; Sommaruga et al., 2012), and low-temperature thermochronological analyses (Cederbom et al., 2004, 2011; Gusterhuber et al., 2012; von Hagke et al., 2012, 2014b; Mazurek et al., 2006).

Studies from the forelands of the European Alps have shown that the most external parts of the orogen were incorporated into the orogenic wedge in Miocene times (e.g. Becker, 2000; Burkhard, 1990; von Hagke et al., 2012, 2014b; Hinsch, 2013; Ortner et al., 2015; Pfiffner, 1986; Schmid et al., 1996; Schönborn, 1992). In the case of the Swiss Molasse Basin, late-Miocene deformation has been kinematically and spatially linked to the uplift and exhumation of the external crystalline massifs (ECMs), which represent basement units derived from the subducting European plate. This late-Miocene deformation stage was also linked to the main deformation in the Jura fold-and-thrust belt (FTB) situated at the northern margin of the Molasse Basin (Figs. 1 and 2; e.g. Boyer and Elliot, 1982; Burkhard, 1990; Burkhard and Sommaruga, 1998; von Hagke et al., 2012; Laubscher, 1961, 1992; Mosar, 1999; Pfiffner, 1986; Sommaruga, 1999). The inferred linkages between the uplift of the ECMs, the imbrication of the proximal molasse deposits, and the main deformation in the Jura FTB are mainly based on a classical scenario of ongoing continent–continent collision, where compressional wedge tectonics and shortening result in crustal thickening of basement units in the hinterland and a propagation of the orogenic wedge towards the foreland, including imbricate thrusting (Pfiffner, 1986; Rosenberg and Berger, 2009; Schmid et al., 1996).

New studies from the Aar Massif of the Central Alps challenge this view. Based on geometric, kinematic, metamorphic, and geodynamic arguments, Herwegh et al. (2017, 2020) suggest that in the eastern ECMs (Aar, Mont Blanc, and Aiguilles Rouges massifs) the mode of uplift and consequentially exhumation switches between "vertical" and "horizontal tectonics". Note that the terms "vertical" and "horizontal tectonics" as used by Herwegh et al. (2017, 2020) are based on geometric and kinematic considerations; i.e. they imply a steeper or less steep orientation of the main faults along which strain is accommodated. Thus, in a compressional framework, these terms describe whether the vertical or the horizontal displacement components play the dominant role at a given point in time. In other words, horizontal shortening also continues during phases of vertical tectonics. The evolution of the Helvetic fold-and-thrust belt with the associated nappe stacking represents an Oligocene stage of horizontal tectonics. A major switch to vertical tectonics occurred in early Miocene times when major parts of the Aar and Mont Blanc–Aiguilles Rouges massifs experienced a strong vertical displacement component mainly along steep to subvertical reverse faults (see Herwegh et al., 2017, 2020, and references therein). This resulted in the differential rock uplift and the doming of these eastern ECMs as well as in a passive upward bulging of the entire nappe stack above. From a geodynamic point of view, (i) a retreating European slab, (ii) delamination of lower crust from the mantle, and (iii) a buoyancy-driven rock uplift component within a compressional regime were suggested by the aforementioned authors to be the driver for this vertical-tectonic forcing. It is important to stress that this vertical displacement component became dominant at a time when the un-thinned or only slightly thinned part of the buoyant former European passive continental margin entered the subduction channel. This stage of vertical tectonics in the eastern ECMs was followed by a second, late-Miocene phase of horizontal tectonics and associated en bloc exhumation (Herwegh et al., 2020), which in the Aar Massif was accomplished through slip along shallow south-dipping basal thrust systems (Berger et al., 2017; Herwegh et al., 2017, 2020; Mair et al., 2018). A similar scenario of a late-stage Miocene en bloc exhumation due to NW-vergent thrusting was proposed for the evolution of the Mont Blanc–Aiguilles Rouges massifs (see Herwegh et al., 2020).

In addition to this ECM-related information, structural, chronostratigraphic, and low-temperature thermochronological data (Burkhard and Sommaruga, 1998; von Hagke et al., 2012, 2014b; Ortner et al., 2015) suggest that the Alpine deformation front remained stationary within the Subalpine Molasse during the time of vertical tectonics. The deformation then propagated to the Jura FTB during the late Miocene when the vertical tectonics was superseded by the thrust-related exhumation in the Aar Massif (e.g. Burkhard and Sommaruga, 1998; von Hagke et al., 2012; Herwegh et al., 2020). The corresponding along-strike partitioning of strain between the Jura FTB and the Subalpine Molasse has, however, only been incompletely resolved so far (e.g. Burkhard, 1990). Likewise, it has been unclear whether the amount of shortening within the Subalpine Molasse is consistent along-strike, particularly with respect to the highly non-cylindrical architecture of the Alpine hinterland as well as the lentoid-shaped map appearance of the eastern ECMs (Fig. 2; Burkhard, 1990). However, this information is vital for understanding how deformation in the ECMs is potentially linked to foreland FTB tectonics. Accordingly, as a first and major contribution of our paper, we aim at reconstructing the chronology and amount of shortening of the molasse sequences during the late stage of Alpine orogeny since the mid-Miocene. We present new low-temperature thermochronological data from the Lake Thun region, which we consider a key area for the understanding of Subalpine Molasse tectonics for the following reasons.

i. With the Aar Massif being one of the best-studied ECM in the Alps in terms of its Alpine tectonic evolution and geodynamic significance, information on the history of thrusting of the Subalpine Molasse in front of the Aar Massif is of great importance if the scope is reconstructing the post-collisional tectonic evolution of the Central Alps.

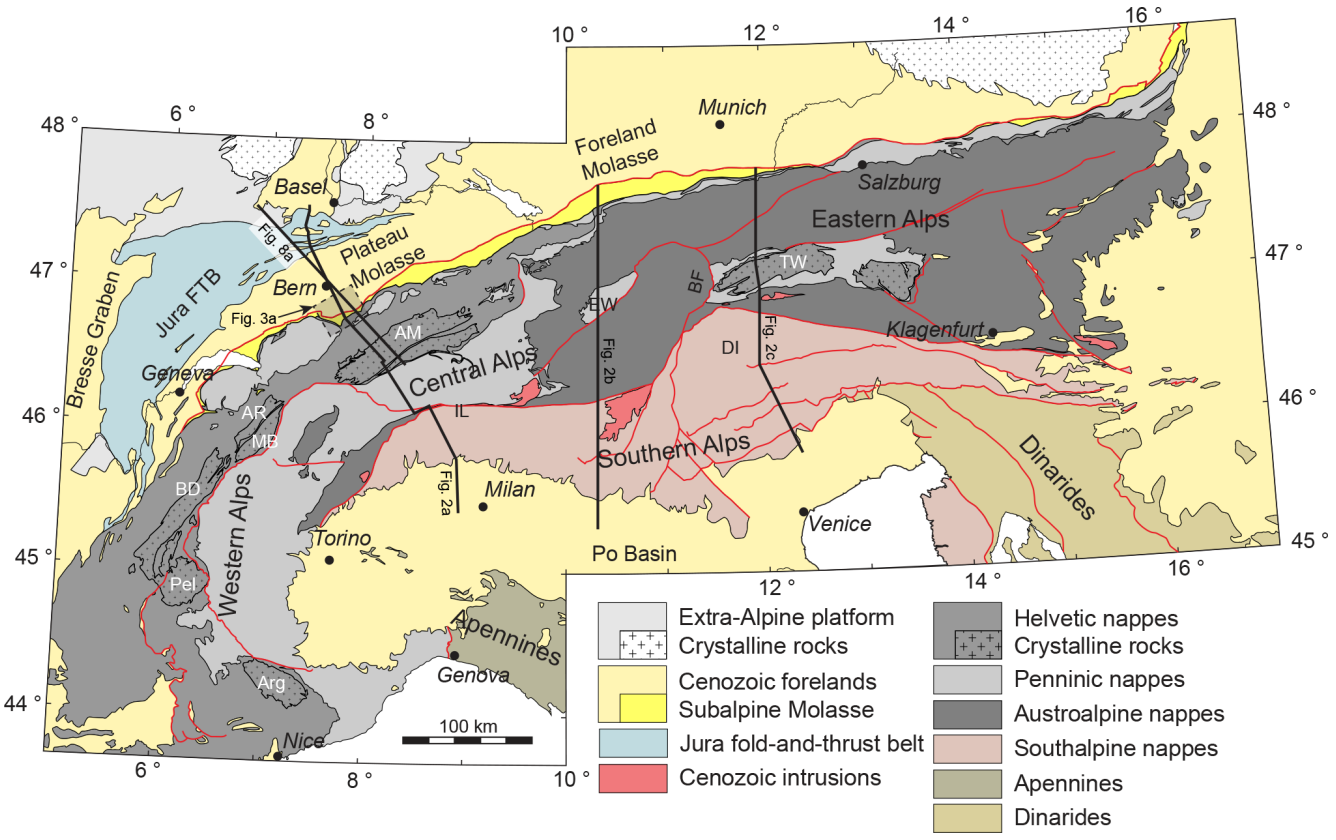

Figure 1. Tectonic map of the European Alps and its foreland basins (adapted from Schmid et al., 2004). Traces of the cross sections in Figs. 2 and 8a are given as bold black lines. The sample area south of Bern (Fig. 3a) is denoted by a dashed rectangle. AM, Aar Massif; AR, Aiguilles Rouges Massif; BD, Belledonne Massif; BF, Brenner Fault; DI, Dolomite indenter; EW, Engadine Window; FTB, fold-and-thrust belt; IL, Insubric Line; MB, Mont Blanc Massif; Pel, Pelvoux Massif; TW, Tauern Window.

ii. The thickness of the basal décollement zone within the Mesozoic cover sediments below the Molasse Basin decreases significantly west of ca. 7° E (Landesgeologie, 2017; Mock and Herwegh, 2017; Sommaruga et al., 2012; Sommaruga et al., 2017). Hence, the Lake Thun area is located in an ideal place where we can expect the eastward transition from the detached Plateau Molasse to the non-detached Foreland Molasse.

iii. While east of the Lake Thun area, the frontal part of the Subalpine Molasse is often delineated by a backthrust and a triangle zone, this feature is largely missing farther west, where predominantly northwestward imbricate thrusting occurs.

We compare the thermochronological data with previously published data from farther east (von Hagke et al., 2012, 2014b). We combine this information with information from well-established work on the chronology, tectonics, and stratigraphy of the thrust Subalpine Molasse between 6.8° E (Lake Geneva) and 12.8° E (near Salzburg; e.g. Burkhard and Sommaruga, 1998; von Hagke et al., 2012, 2014b; Hinsch, 2013; Kempf et al., 1999; Ortner et al., 2015; Pfiffner, 1986; Schlunegger et al., 1997; and many others) in order to better constrain the timing and spatial pattern of thrusting in the Subalpine Molasse. We will relate this to the history of shortening of the Jura FTB and to Alpine tectonic events in an effort to identify possible relationships with the geodynamic forcing at a larger scale.

Geological mapping of the Subalpine Molasse (e.g. Ganss and Schmidt-Thomé, 1953; Haldemann et al., 1980; Schlunegger et al., 2016; Weidmann et al., 1993; Zaugg et al., 2011) as well as stratigraphic work (e.g. Bachmann and Müller, 1992; Kempf et al., 1999; Lemcke, 1988; Schlunegger et al., 1993, 1997; Schlunegger and Kissling, 2015) has shown that the proximal basin border is characterized by large orogen-parallel lithologic variations where kilometer-thick conglomerate suites with high mechanical strengths alternate with mudstones and sandstones with low at-yield conditions over lateral distances of a few kilometers. As a consequence, the patterns of thrust faults and folds within the Subalpine Molasse change along-strike. In regions where kilometer-thick conglomerate packages are present, the geometry of the Subalpine Molasse is characterized by kilometer-spaced thrust faults with relatively large

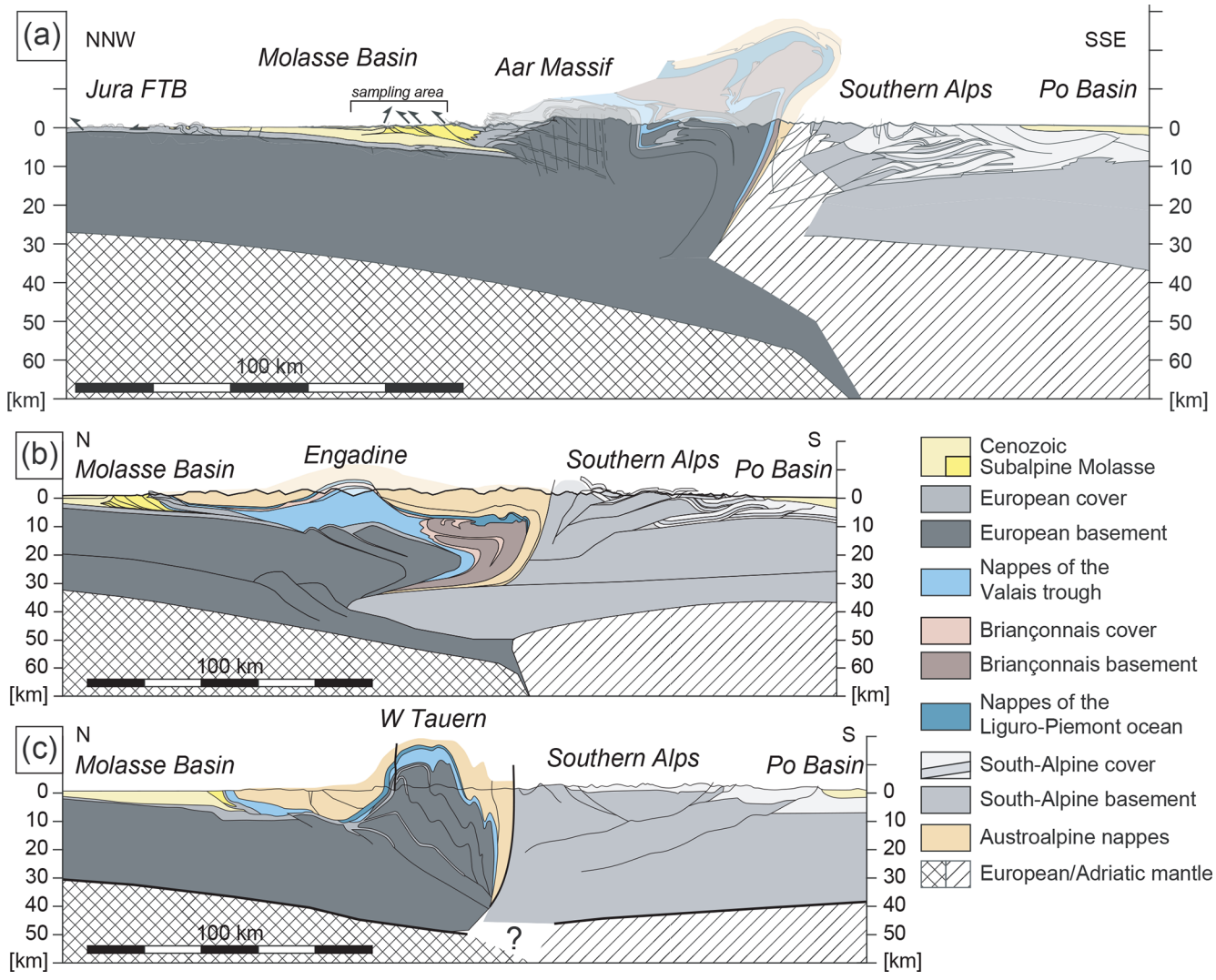

Figure 2. Cross sections through the Alps. **(a)** Jura – Plateau Molasse – Aar Massif (compiled from Buxtorf, 1916; Herwegh et al., 2017; Mock and Herwegh, 2017; Pfiffner, 2009; Rosenberg and Kissling, 2013). **(b)** Engadine Window (adapted from Rosenberg et al., 2015). **(c)** Western Tauern Window (adapted from Rosenberg et al., 2015).

displacements on them (e.g. Ortner et al., 2015; von Hagke et al., 2012, 2014b). In areas however, where the foreland mechanical stratigraphy mainly consists of sandstone–mudstone alternations, the structural style is characterized by closely spaced folds and thrust faults with possibly smaller displacements (e.g. Kempf et al., 1999; Ortner et al., 2015; Schlunegger et al., 1993, 1997). We expect that these differences in mechanical stratigraphy leave an imprint on where strain was accommodated during late orogenic shortening. Therefore, as a related second contribution, we aim at exploring how lithological variations within the foreland basin, which were controlled by the paleogeographic conditions, contributed to the spatial distribution of late orogenic strain.

2 Geological and tectonic setting

2.1 The Central Alps

Classically, the boundary (or transition) between the Central and the Eastern Alps has been located in eastern Switzerland (e.g. Schmid et al., 2004). There, remnants of the Piemont–Ligurian Ocean separate units of European origin (Central and Western Alps) from thrust nappes that are part of the Adriatic continental plate (Figs. 1 and 2; Eastern Alps; Schmid et al., 2004). However, this surface observation is not reflected in the slab geometry at depth. Instead, seismotomography studies have shown that the subducting European slab beneath the Central Alps extends to the east until ca. 11–13° E, i.e. between the Giudicarie–Brenner fault system and the central Tauern Window, where a segmenta-

tion of the slab structure is observed (Hetényi et al., 2018b; Kästle et al., 2020; Lippitsch et al., 2003; Mitterbauer et al., 2011; Zhao et al., 2016; see further details in the "Discussion" section). Similar to Rosenberg et al. (2018), who place the boundary between the Central and Eastern Alps at the Giudicarie–Brenner fault system, we shift this boundary farther east than classically placed (e.g. Schmid et al., 2004). We thus follow the argumentation given above, which is also advocated by Kissling and Schlunegger (2018), and place the Central Eastern Alps transition where the current slab configuration changes at depth. This is particularly important when the influence of subduction mechanisms on the surface geology during the past few millions of years is considered, which is the scope of the discussion of the results at the end of this paper. In this study, we therefore focus on the Central Alps because late-Miocene thrusting in the Subalpine Molasse terminates near Salzburg (Fig. 1; Beidinger and Decker, 2014; Hinsch, 2013; Ortner et al., 2015), thus spatially coinciding with the aforementioned along-strike changes in the configuration of the lithospheric mantle slabs at depth between ca. 11 and 13° E. However, we will elaborate on the influences of Eastern Alpine tectonic processes in the discussion part of this paper.

The Central Alps are situated almost entirely on top of the subducted Central European lithospheric slab (Fig. 2a and b; Schmid et al., 2017), which steeply dips into the asthenospheric mantle as imaged by teleseismic tomography (Lippitsch et al., 2003). The orogen is the result of the Late Cretaceous to Eocene subduction of the oceanic part of the European plate under the Adriatic continental plate and subsequent post-35 Ma continent–continent collision (e.g. Schmid et al., 1996). Subduction initially affected the European oceanic lithosphere, which was followed by the subduction of the distal spur of the Iberian plate that became the Penninic thrust nappes. During the Eocene, subduction started to involve the distal and stretched European continental margin (e.g. Cardello et al., 2019; Mosar et al., 1996; Stampfli and Marchant, 1997). The subduction system then became clogged when the thick and buoyant European crust started to enter the subduction channel. As a result, the subducted oceanic slab of the European plate supposedly broke off, which has been inferred from widespread plutonism ca. 32 Myr ago (Davies and von Blanckenburg, 1995). Slab unloading and basal accretion of crustal segments to the upper plate resulted in rock and surface uplift. This gave way to the incipient rise of the Alpine topography and consequently exhumation of uplifted rocks. Uplift was mainly accomplished through backthrusting along the Insubric Line (Hurford, 1986; Schmid et al., 1996), and this was also manifested in the increase in sediment discharge into the Alpine foreland (Schlunegger and Castelltort, 2016; Sinclair, 1997).

During the Oligocene, Europe-derived sedimentary units were sheared off from their substratum and emplaced to the north over a distance of several tens of kilometers, thereby forming the present-day Helvetic cover nappes (Pfiffner, 2011, and references therein). Ongoing convergence resulted in delamination of lower European crustal segments from the lithospheric mantle (Fry et al., 2010). This mechanism eventually resulted in the inferred buoyancy-driven subvertical uplift of the thickened crust (Kissling and Schlunegger, 2018) along steeply dipping shear zones and in the exhumation of the ECMs ca. 20 Myr ago (Fig. 2a; e.g. Egli et al., 2017; Glotzbach et al., 2011; Herwegh et al., 2017, 2020). Farther east, between the Aar Massif and the Brenner Fault (a segment, which we here regard as the eastern Central Alps), such Europe-derived crustal blocks are not exposed at the surface. East of the Brenner Fault (Fig. 1), northward indentation of the Adriatic plate resulted in eastward-directed lateral extrusion of crustal blocks, which started in early Miocene times (Frisch et al., 1998; Handy et al., 2015; Ratschbacher et al., 1991). This process was associated with the exhumation of the Tauern Window, which was accomplished by upward folding and erosion of the nappe pile and by normal faulting along its bounding low-angle normal faults (see Rosenberg et al., 2018, and references therein).

Late stages in the evolution of the Central Alps are dominated by orogen-perpendicular growth when the deformation front of the Alps propagated to the external parts, resulting in the development of the Jura FTB and the Subalpine Molasse in the north and in the ongoing growth of the Southern Alps on the southern side of the Alps (Figs. 1 and 2; Burkhard, 1990; Caputo et al., 2010; Castellarin and Cantelli, 2000; Nussbaum, 2000; Pfiffner, 1986; Schmid et al., 1996; Schönborn, 1992).

2.2 The Molasse Basin

2.2.1 Structures and tectonic evolution

The Molasse Basin of the north Alpine foreland, which contains deposits derived from the progressive erosion of the evolving Alps since 32 Ma (Sinclair et al., 1991), can tectonically be subdivided into three parts. (i) The Plateau Molasse is the gently folded part of the basin, which evolved into a wedge-top basin (e.g. Willett and Schlunegger, 2010) during the late Miocene when the Jura FTB experienced its major phase of deformation. Folding of the Jura FTB was accomplished as the Mesozoic suite of limestones and marls became detached from the underlying basement along a main décollement zone within the Triassic evaporites. To the east, with the Triassic evaporites diminishing and the Jura FTB tapering off, the basin gradually changes into a non-detached configuration, (ii) the Foreland Molasse (e.g. Berge and Veal, 2005; Ortner et al., 2015; Pfiffner, 1986). At the southern, proximal basin border, (iii) the Subalpine Molasse extends continuously as a narrow band of imbricates from south of Geneva to Salzburg, where it disappears beneath Helvetic and Penninic units before it emerges again in upper Austria. In this contribution we mainly focus on the Subalpine Molasse between Lake Geneva and Salzburg, i.e. the part of the

fold–thrust belt where the tectonic processes may be associated with the subduction of the European lithospheric slab of the Central Alps.

The Subalpine Molasse consists of south-dipping imbricated thrust sheets. In large parts and predominantly northeast of the Lake Thun area, the structures of the Subalpine Molasse also include the north-dipping backthrusts that form a triangle zone at the transition to the Plateau and Foreland Molasse (Fig. 2; Berge and Veal, 2005; Fuchs, 1976; Müller et al., 1988; Ortner et al., 2015; Schuller et al., 2015; Sommaruga et al., 2012). The Subalpine Molasse started to become incorporated into the orogenic wedge shortly after deposition in Oligocene times (Hinsch, 2013; Kempf et al., 1999; Pfiffner, 1986). After ca. 20 Ma, contemporaneously with the development of the frontal triangle zone, the northern Alpine thrust front remained stationary in the area of the Subalpine Molasse (Burkhard and Sommaruga, 1998; von Hagke et al., 2014b; Ortner et al., 2015). It was not until ca. 12 Ma when parts of the deformation in the western Molasse Basin (i.e. west of Lake Constance) propagated along a basal décollement zone within the Triassic evaporites into the thin-skinned Jura FTB (Becker, 2000; Burkhard and Sommaruga, 1998; Laubscher, 1961; Philippe et al., 1996), although some deformation occurred already in the late Oligocene in the area of today's Jura FTB (Aubert, 1958; Liniger, 1967). Hence, during the late Miocene, the Molasse Basin experienced along-strike changes in tectonic style and locus of deformation. While sediment accumulation in the eastern Molasse Basin (i.e. here the Foreland Molasse between Lake Constance and Salzburg) still occurred in a foredeep setting, at this stage the western part evolved into a wedge-top basin (i.e. Plateau Molasse; Willett and Schlunegger, 2010). Both the evaporite basal décollement and the thrusts of the Subalpine Molasse are considered to root below and in the ECMs. Accordingly, they were kinematically linked to the late-Miocene exhumation of the ECMs (Fig. 2a; e.g. Burkhard, 1990), which was driven at that time by north-directed thrusting along shallow-dipping faults (Herwegh et al., 2017, 2020), thereby causing a phase of accelerated exhumation at ca. 10 Ma (Fox et al., 2016; Glotzbach et al., 2010; Valla et al., 2012; Vernon et al., 2009; Weisenberger et al., 2012). Based on stratigraphic data, Haus (1935) inferred already in 1935 that the Subalpine Molasse of Central Switzerland was subject to major thrusting in late-Miocene times. Recently, studies have revisited this topic and documented that the Subalpine Molasse was subject to break-back thrusting between ca. 13 and 4 Ma (von Hagke et al., 2012, 2014b; Ortner et al., 2015; Schuller et al., 2015), which was thus coeval to folding and thrusting in the Jura FTB. We note that late-Miocene thrusting is not recorded in the Subalpine Molasse east of Salzburg (Beidinger and Decker, 2014; Hinsch, 2013; Ortner et al., 2015).

After 10 Ma, but possibly as late as 5 Ma, the entire Molasse Basin was uplifted, resulting in basin-scale erosion (Baran et al., 2014; Cederbom et al., 2004, 2011; Genser et al., 2007; Gusterhuber et al., 2012; von Hagke et al., 2012; Mazurek et al., 2006; Schlunegger and Mosar, 2011; Zweigel et al., 1998). Since 5 Ma, compressional thin-skinned tectonics in the wedge-top part of the basin and the Jura FTB are superseded by thick-skinned tectonics (Giamboni et al., 2004; Guellec et al., 1990; Madritsch et al., 2008; Mock and Herwegh, 2017; Mosar, 1999; Philippe et al., 1996; Ustaszewski and Schmid, 2007).

2.2.2 Stratigraphic development

The clastic infill of the Oligocene to Miocene peripheral Molasse Basin consists of eroded sediments of the evolving Alps and in the northern parts partly of material shed from the Black Forest and the Bohemian Massif. Accommodation space was formed through subsidence, classically related to flexural bending of the European plate in response to the combined effect of subsurface slab loading and topographic loading of the advancing Alpine thrust wedge during Paleogene and Neogene times (Allen et al., 1991; Burkhard and Sommaruga, 1998; Karner and Watts, 1983; Pfiffner, 1986; Zweigel et al., 1998). For the Central Alps, this view has recently been challenged by Schlunegger and Kissling (2015), who favor a slab rollback mechanism to explain foreland plate flexure and accommodation space formation. In this scenario, slab rollback is driven by the interplay between vertically directed slab loads exerted by the subducted European lithospheric mantle and buoyancy-driven crustal delamination (Kissling and Schlunegger, 2018).

In the Swiss part of the basin, the molasse sediments form two regressive and coarsening-upward megasequences (Homewood et al., 1986; Kuhlemann and Kempf, 2002; Schlunegger et al., 2007). The first megasequence describes the transition from Rupelian (ca. pre-30 Ma) sedimentation in underfilled conditions to Chattian–Aquitanian (ca. 28–20 Ma) sedimentation when the basin was overfilled. The Burdigalian (ca. 20–17 Ma) and post-Burdigalian (ca. post-17 Ma) stratigraphic records then chronicle the second megasequence during filled to overfilled conditions (Sinclair and Allen, 1992). West of ca. 11° E, large alluvial megafans developed at the mountain front during the overfilled stage of the basin (Frisch et al., 1998; Kuhlemann and Kempf, 2002; Ortner et al., 2015). At their cores, close to the apex, large and kilometer-thick conglomerate sequences were deposited, while at the margins, the sedimentation was mainly sand- and mudstone dominated. At the proximal basin border, numerous locally derived torrents resulted in the construction of bajada fans, which further contributed to the high along-strike stratigraphic variability at the proximal basin border (Kempf et al., 1999; Schlunegger et al., 1997; Spiegel et al., 2001). Farther east, the Molasse Basin prevailed in an underfilled stage until at least 17 Ma, when sedimentation of sandstones and marls occurred under brackish to shallow marine conditions (Hinsch, 2013; Kuhlemann and Kempf, 2002; Lemcke, 1988; Ortner et al., 2015). Large alluvial fans are

missing due to the channelizing effect of the paleo-Inn river, which transported the erosional detritus effectively farther to the east (Frisch et al., 1998; Kuhlemann and Kempf, 2002). For more details on the laterally varying stratigraphy, including Wheeler diagrams, the reader is referred to Kempf et al. (1999), Schlunegger et al. (1997), and Schlunegger and Norton (2013) as well as Hinsch (2013), Kuhlemann and Kempf (2002), Lemcke (1988), and Ortner et al. (2015) for the Molasse Basin west and east of Lake Constance, respectively.

2.3 Litho-tectonic architecture of the Lake Thun area

In the sampling area, mapping shows that the litho-tectonic architecture of the Subalpine Molasse contrasts between both sides of Lake Thun (Fig. 3; Beck, 1945; Blau, 1966; Haus, 1937; Jordi, 2012; Landesgeologie, 2005; Mock and Herwegh, 2017; Rutsch, 1947; Schlunegger et al., 1993, 1997; Vollmayr, 1992). On the eastern side, the basin is generally made up of amalgamated conglomerates, which are cut from west to east by two narrow sand- and mudstone-dominated bands. The south-dipping thrust north of the Falkenfluh anticline as well as the three tightly spaced thrusts further south all emerge along these mechanically weaker bands (Fig. 3a). In between these thrust domains, we observe large tectonic slices (6–8 km wide) made up of mechanically strong conglomerates of Burdigalian (north) and Chattian–Aquitanian age (south). The latter is bordered to the north by three thrusts for which we can infer a break-back (i.e. back-stepping) sequence of thrusting from cross-cutting relationships in map view (Fig. 3a). To the south, across a south-dipping thrust, Rupelian sand- and mudstones crop out. West of the Aar valley, conglomerates are largely absent and the stratigraphy is sand- and mudstone dominated. Compared to the Subalpine Molasse east of the Aar valley, the FTB is much narrower, thrusts are more evenly distributed, and the tectonic slices are narrower (2–3 km; Fig. 3). Across the whole area we can see a clear correlation between the distribution of mechanically weak sand- and mudstones and the location and alignment of thrust faults. The subsurface continuation of the thrusts has been inferred from seismic interpretation (for more details, see Mock and Herwegh, 2017), which suggests that the thrusts merge in a detachment level at a depth of ca. 2 km (Fig. 3b). However, the type of lithology of the detachment remains unknown, since the poor signal-to-noise ratio of the seismic images does not allow a clear distinction in this regard. Due to the lack of subsurface data further south it also remains speculative how the structures extend southward. As indicated in the sections (Fig. 3b), it is, however, likely that the thrusts root within the Rupelian sand- and mudstones at the base of the molasse sequence on top of the Mesozoic cover sediments. In summary, there are pronounced differences both in the mechanical stratigraphy as well as in the structural configuration of the Subalpine Molasse west and east of the Aar valley. We discuss this in detail in Sect. 5.1 below.

3 Methods

3.1 Selection of sample sites and litho-tectonic architecture

We collected 12 samples across the Subalpine Molasse east and west of Lake Thun for apatite (U−Th−Sm)/He (AHe) dating (Fig. 3). The northernmost samples represent coarse-grained Burdigalian sandstones of the Plateau Molasse. Further to the southwest, we sampled Chattian–Aquitanian and Rupelian sandstones within the Subalpine Molasse. Samples have been collected in the hangingwalls and footwalls of the individual thrusts (Fig. 3). To control the depositional age of the sediments, samples were taken in the vicinity of sites with known mammal ages and magneto-polarity-based chronologies (Schlunegger et al., 1996; Strunck and Matter, 2002) wherever possible. In order to test the influence of along-strike changes in the mechanical stratigraphy of the Subalpine Molasse on the thrusting pattern, we compiled more details about the geological architecture of the proximal molasse from published geological maps (Landesgeologie, 2005) and use available tectonic sections (Ortner et al., 2015; Sommaruga et al., 2012) to illustrate the related tectonic style.

3.2 (U−Th−Sm)/He (AHe) thermochronology and thermal modeling

We determined the most recent exhumation history of the Subalpine Molasse of the Lake Thun region through AHe dating. This method is based on the α decay of ^{238}U, ^{235}U, ^{232}Th, and ^{147}Sm isotopes and the retention of the radiogenic product ^{4}He in the crystal lattice below a certain temperature (e.g. Farley, 2002). Diffusive loss of ^{4}He in the lattice depends on the grain size, shape, chemical composition, distribution of the mother isotopes, radiation damage density, and the time–temperature evolution of the crystal (Farley, 2002; Wolf et al., 1996). Consequently, AHe ages can provide estimates for about the time when the mineral passed through the diffusion-sensitive temperature interval between ca. 80 and 40 °C (Wolf et al., 1996), which is referred to as the partial retention zone (PRZ). Hence, this method allows constraining the tectono-thermal history of the studied rocks in the uppermost few kilometers of Earth's crust. Detrital apatite grains deposited in sedimentary basins primarily carry a cooling history of the hinterland at the time of erosion. Subsequent burial due to sedimentation or tectonic loading may reheat the detrital grains to temperatures above the closure temperature, thereby resetting the chronometer. Subsequent exhumation will chronicle the basin's exhumation, whereas grains that have not been reset during the basin's burial history still carry a signal of older cooling events. Consequently,

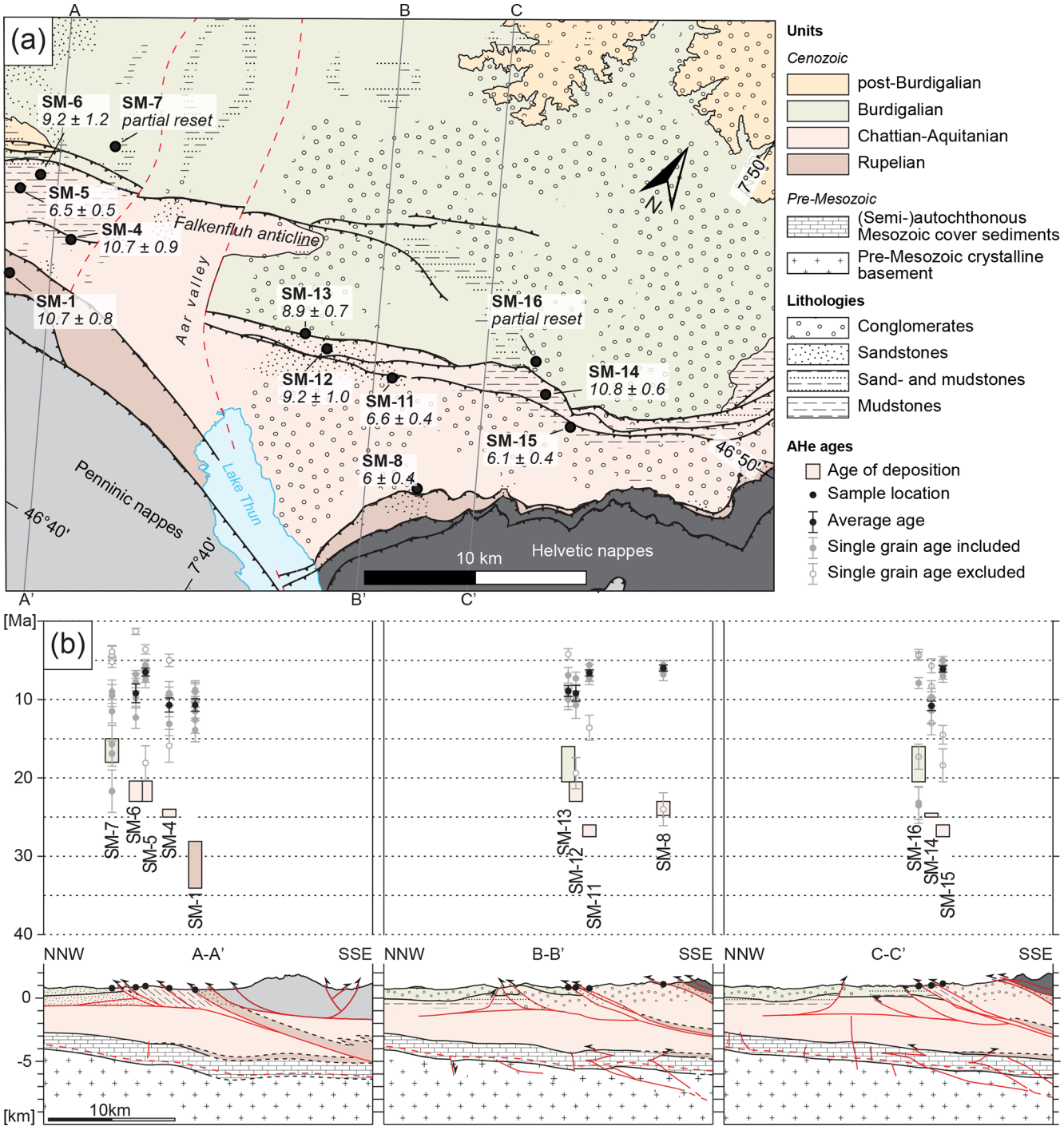

Figure 3. (a) Litho-tectonic map of the Lake Thun area showing sample locations and corresponding average apatite (U−Th−Sm)/He (AHe) ages. Traces of cross sections A–A', B–B', and C–C' in Fig. 3b are given as black lines. The location of the sampling area is shown as a dashed rectangle in Fig. 1. Note the arrow indicating north. **(b)** Cross sections through the sampling area west (A–A') and east of the Aar valley (B–B' and C–C'), showing single-grain and average AHe ages. Tectonic information is based on Beck (1945), Haus (1937), Jordi (2012), Mock and Herwegh (2017), Rutsch (1947), and Schlunegger et al. (1993, 1997). Lithological information is compiled from Landesgeologie (2005) and Schlunegger et al. (1993).

the relation between cooling age and stratigraphic age may provide estimates on the burial as well as the exhumation history (e.g. Reiners and Brandon, 2006).

We used a combination of standard techniques for the separation of apatite minerals, which particularly includes electrodynamic disaggregation, and magnetic and heavy liquid separation. Single crystals were handpicked under a binocular and checked for inclusions and imperfections under an optical microscope with cross-polarized light (more information on the mineral separation techniques and picking criteria are given in Sect. S1 in the Supplement). Helium extraction and measurement of parent isotope contents has been conducted at the GÖochron laboratories of the University of Göttingen. Raw ages were corrected for α ejection (Table 1). We measured four to eight single-grain ages per sample and calculated average ages using the unweighted arithmetic mean for completely reset samples. We excluded single-grain ages for subsequent geological interpretation based on the following criteria (Table 1): (i) high analytical errors ($> 10\,\%$), (ii) very low U content (< 10 ppm), (iii) a substantial amount of He on the first re-extract ($> 4\,\%$), or (iv) erroneous old ages stemming most likely from U−Th-rich mineral inclusions which produce parentless He. For the latter case, we plotted the He content versus the present-day He production rate in order to detect these ages (for details, see Vermeesch, 2008).

We constrained the thermal histories of the sampled sediments (Fig. 4) by modeling the AHe age data with the HeFTy software (Ketcham, 2005). We gave the algorithm a high degree of freedom by using only a few modeling constraints: the age of sedimentation, the paleo-temperature (Mosbrugger et al., 2005), the present-day annual average temperature, and maximum post-depositional heating rates inferred from maximum sedimentation rates (Schlunegger and Norton, 2015) and a paleo-geothermal gradient of $28\,^{\circ}\mathrm{C\,km^{-1}}$ (Schegg and Leu, 1998).

4 Results

4.1 AHe age data

Samples SM-7 and SM-16 from the Plateau Molasse show a wide spread in AHe ages, indicating a partially exhumed fossil PRZ. Hence, they did not experience enough post-depositional heating for a full reset of the thermochronometer (Fig. 3b and Table 1). All other samples show single-grain ages, which plot within error for each sample. Ages are significantly younger than the corresponding depositional ages and are thus considered to represent completely reset ages (fully exhumed fossil PRZ), hence inferring substantial post-depositional burial and heating.

Average ages for completely reset samples range from 6.0 ± 0.4 to 10.8 ± 0.6 Ma (Fig. 3b and Table 1). All samples from the Subalpine Molasse show post-depositional burial and heating to $> 60\,^{\circ}\mathrm{C}$ (Fig. 4). Sample SM-7 from the Plateau Molasse did not experience enough post-depositional heating to fully reset the thermochronometer (Fig. 4). Thermal modeling supports the young exhumation of the Subalpine Molasse between 12 and 5 Ma (Fig. 4). The thermal histories of SM-7 and SM-13 indicate an exhumation signal of the Plateau Molasse at ca. 10 Ma.

Samples SM-8, SM-11, and SM-15 were collected from the same tectonic sliver (Figs. 3a and 5), and corresponding average ages of 6.0 ± 0.4, 6.6 ± 0.4, and 6.1 ± 0.4 Ma group well within their margins of error. A jump in average ages occurs across the thrust to the adjacent tectonic slivers and the Plateau Molasse in the north, where samples SM-12, SM-13, and SM-14 yield average ages of 9.2 ± 1, 8.9 ± 0.7, and 10.8 ± 0.6 Ma, respectively, thus also grouping within their margins of error. This pattern is also reproduced by the modeled thermal histories, where a jump in exhumation ages across tectonic boundaries is recognized (Fig. 4). In the western area, the average ages do not show such a close correlation with the tectonic position (Figs. 3a and 5). However, the thermal models for samples SM-5 and SM-6 indicate younger cooling than for samples SM-4 and SM-7 (Fig. 4), thus suggesting a tectonic control on exhumation.

4.2 Late-Miocene shortening estimates

Based on published restored cross sections (Burkhard and Sommaruga, 1998; von Hagke et al., 2014b; Ortner et al., 2015), retro-deformed and balanced palinspastic maps (Philippe et al., 1996), thermochronological data (von Hagke et al., 2012, 2014b), and our own cross section restorations (see Sect. S2 and Fig. S1 in the Supplement), we estimated the amount of late-Miocene horizontal shortening of the Subalpine Molasse and the Jura FTB from Lake Geneva to Salzburg (Fig. 6b). Post-12 Ma horizontal shortening in the Jura FTB decreases from a maximum of ca. 32 km in the west to 0 km at the eastern tip (Philippe et al., 1996). Contrariwise, minimum horizontal shortening in the Subalpine Molasse increases from ca. 10 km in the west (Lake Geneva) to ca. 20 km farther east (Lake Constance) before decreasing again to below 1 km in the area near Salzburg (Beidinger and Decker, 2014; Burkhard and Sommaruga, 1998; von Hagke et al., 2012, 2014b; Hinsch, 2013; Ortner et al., 2015). These values do not account for the shortening taken up by the frontal triangle zone between ca. 20 Ma and 12 Ma (von Hagke et al., 2014b; Kempf et al., 1999; Ortner et al., 2015). We acknowledge that shortening estimates for the Subalpine Molasse are subject to uncertainties (Burkhard and Sommaruga, 1998; von Hagke and Malz, 2018; Ortner et al., 2015) and likely represent minimum estimates due to (i) the unconstrained large parts of proximal Subalpine Molasse, which are hidden below the frontal thrusts of the Helvetic nappes and Penninic Klippen units, and (ii) the non-preservation of the hangingwall cut-offs of individual thrust sheets. Despite these uncertainties, we observe that the late-

Table 1. Apatite (U−Th−Sm)/He dating results.

Sample	He vol. (ncc)[a]	1σ (%)	U mass (ng)	1σ (%)	Th mass (ng)	1σ (%)	Sm mass (ng)	1σ (%)	Ft[b]	Raw age (Ma)	Corrected age (Ma)	2σ (Ma)[c]	Average age (Ma)[d]	2 SD error (Ma)[e]	Excluded age[f]
SM-1 a1	0.02	3.77	0.01	5.64	0.07	2.56	0.34	7.06	0.60	5.5	9.0	1.4			
SM-1 a2	0.08	2.09	0.04	2.66	0.21	2.45	0.98	6.92	0.72	7.2	10.0	1.0			
SM-1 a4	0.07	2.43	0.03	3.18	0.15	2.47	0.66	6.84	0.74	8.5	11.5	1.2			
SM-1 a5	0.03	3.70	0.02	4.97	0.07	2.56	0.40	7.15	0.69	6.2	9.0	1.2			
SM-1 a6	0.08	2.09	0.03	2.52	0.15	2.45	0.55	3.47	0.68	9.4	13.9	1.5			
SM-1 a7	0.05	2.67	0.02	3.25	0.14	2.46	0.92	3.64	0.79	6.9	8.8	0.8			
SM-1 a8	0.04	3.24	0.03	2.65	0.02	2.82	0.23	3.34	0.64	8.1	12.6	1.7	10.7	0.8	
SM-4 a1	0.03	3.13	0.02	3.08	0.01	2.48	0.03	3.70	0.66	10.5	15.9	2.1			e
SM-4 a2	0.06	2.51	0.06	2.03	0.10	2.42	0.37	3.70	0.61	5.9	9.6	1.2			
SM-4 a3	0.01	4.81	0.02	3.79	0.05	2.49	0.56	3.70	0.59	3.0	5.0	0.8			e
SM-4 a4	0.06	2.64	0.05	2.20	0.06	2.45	0.51	3.70	0.61	6.6	10.8	1.4			
SM-4 a5	0.02	4.31	0.02	3.99	0.03	2.54	0.34	3.70	0.55	5.0	9.2	1.5			
SM-4 a6	0.08	2.21	0.07	2.01	0.02	2.64	0.38	3.70	0.66	8.6	13.1	1.5	10.7	0.9	
SM-5 a1	0.05	2.79	0.04	2.52	0.13	2.46	0.90	3.70	0.62	4.7	7.5	1.0			
SM-5 a2	0.10	2.11	0.15	1.86	0.09	2.43	0.66	3.70	0.66	4.6	7.0	0.8			
SM-5 a3	0.02	4.42	0.02	4.25	0.06	2.57	0.25	3.70	0.74	4.3	5.8	0.7			
SM-5 a4	0.01	5.90	0.01	6.10	0.09	2.50	0.22	3.70	0.62	2.2	3.6	0.6			e
SM-5 a5	0.04	3.02	0.04	2.35	0.15	2.46	1.00	3.70	0.65	3.7	5.6	0.7			
SM-5 a6	0.20	1.51	0.13	1.88	0.08	2.44	0.54	3.70	0.63	11.3	18.1	2.2	6.5	0.5	e
SM-6 a1	0.05	2.66	0.05	2.20	0.10	2.43	0.83	3.70	0.61	6.0	9.8	1.3			
SM-6 a2	0.07	2.20	0.07	2.04	0.12	2.47	1.30	3.70	0.82	5.6	6.8	0.5			
SM-6 a3	0.04	2.90	0.04	2.29	0.08	2.44	0.77	3.70	0.61	4.8	7.8	1.1			
SM-6 a4	0.00	9.84	0.00	43.45	0.01	2.77	1.05	3.70	0.59	0.8	1.3	0.4			e
SM-6 a5	0.14	1.72	0.13	1.87	0.02	2.68	0.51	3.70	0.64	7.9	12.3	1.4	9.2	1.2	
SM-7 a1	0.01	7.55	0.01	5.93	0.03	2.67	0.34	4.55	0.54	2.1	3.9	0.8			e
SM-7 a2	0.03	3.57	0.02	3.57	0.02	2.88	0.43	3.21	0.69	7.9	11.5	1.5			
SM-7 a3	0.15	1.66	0.07	2.00	0.07	2.52	0.31	4.06	0.62	13.5	21.7	2.7			
SM-7 a4	0.02	4.43	0.02	4.16	0.04	2.62	0.31	3.52	0.57	5.1	9.0	1.5			
SM-7 a5	0.05	2.85	0.03	2.82	0.05	2.58	0.41	3.81	0.54	8.4	15.7	2.4			
SM-7 a6	0.02	4.37	0.02	3.98	0.05	2.45	0.57	3.70	0.71	3.7	5.2	0.7			e
SM-7 a7	0.02	4.28	0.01	6.31	0.04	2.65	0.60	3.70	0.65	6.1	9.5	1.4			
SM-7 a8	0.24	1.48	0.13	1.87	0.11	2.42	0.57	3.70	0.73	12.3	16.9	1.6			
SM-7 a9	0.00	8.62	0.00	28.40	0.03	2.69	0.30	3.70	0.55	2.4	4.3	1.1			e
SM-8 a1	0.02	3.67	0.02	3.39	0.06	2.54	0.56	4.01	0.77	4.4	5.7	0.6			
SM-8 a2	0.02	3.68	0.03	3.02	0.03	2.67	0.43	4.57	0.70	4.7	6.8	0.8			
SM-8 a3	0.12	1.93	0.03	2.61	0.08	2.50	0.56	3.86	0.77	18.5	24.0	2.1			e
SM-8 a4	0.02	3.88	0.02	3.25	0.06	2.55	0.53	3.32	0.80	4.5	5.6	0.6	6.0	0.4	
SM-11 a1	0.05	2.53	0.05	2.14	0.11	2.42	0.47	4.56	0.78	5.5	7.0	0.6			
SM-11 a2	0.02	4.35	0.02	3.89	0.06	2.45	0.34	3.42	0.73	5.3	7.2	0.9			
SM-11 a3	0.02	4.04	0.02	4.02	0.07	2.43	0.52	3.68	0.75	4.1	5.6	0.7			
SM-11 a4	0.02	4.77	0.02	3.77	0.06	2.44	0.30	4.20	0.57	3.8	6.6	1.1			
SM-11 a5	0.05	2.52	0.04	2.35	0.04	2.49	0.26	4.54	0.67	9.2	13.6	1.6	6.6	0.4	e
SM-12 a1	0.04	3.00	0.04	2.22	0.06	2.44	0.40	3.80	0.51	5.5	10.7	1.7			
SM-12 a2	0.26	1.50	0.15	1.84	0.01	2.72	0.46	4.13	0.69	13.4	19.4	2.0			e
SM-12 a3	0.02	3.63	0.03	2.85	0.03	2.51	0.36	3.46	0.74	5.4	7.3	0.8			
SM-12 a4	0.22	1.50	0.19	1.83	0.18	2.41	0.46	4.07	0.82	7.8	9.6	0.7	9.2	1.0	
SM-13 a1	0.06	2.27	0.07	1.99	0.02	2.84	0.59	3.13	0.61	6.1	10.0	1.3			
SM-13 a2	0.04	2.93	0.03	2.54	0.04	2.67	0.39	3.93	0.68	6.6	9.7	1.2			
SM-13 a3	0.06	2.59	0.07	2.05	0.01	3.46	0.35	4.68	0.74	6.8	9.1	0.9			
SM-13 a4	0.02	4.51	0.02	2.96	0.02	2.71	0.31	4.28	0.63	4.3	6.9	1.0			
SM-13 a5	0.01	6.37	0.01	5.91	0.01	2.82	0.34	3.96	0.76	3.2	4.2	0.7	8.9	0.7	e

Table 1. Continued.

Sample	He vol. (ncc)[a]	1σ (%)	U mass (ng)	1σ (%)	Th mass (ng)	1σ (%)	Sm mass (ng)	1σ (%)	Ft[b]	Raw age (Ma)	Corrected age (Ma)	2σ (Ma)[c]	Average age (Ma)[d]	2 SD error (Ma)[e]	Excluded age[f]
SM-14 a1	0.06	2.60	0.03	2.71	0.06	2.44	0.55	3.70	0.68	8.9	13.0	1.5			e
SM-14 a2	0.03	3.33	0.02	3.21	0.07	2.44	0.39	3.70	0.56	6.4	11.4	1.7			
SM-14 a3	0.05	2.66	0.03	2.70	0.10	2.48	0.32	3.70	0.59	6.8	11.4	1.6			
SM-14 a4	0.02	4.41	0.02	3.66	0.05	2.62	1.11	3.70	0.61	3.4	5.7	0.9			e
SM-14 a5	0.04	3.07	0.02	3.59	0.07	2.53	0.41	3.70	0.73	7.1	9.7	1.1			
SM-14 a6	0.07	2.25	0.05	2.10	0.09	2.43	2.20	3.70	0.79	6.5	8.3	0.7	10.8	0.6	e
SM-15 a1	0.04	2.72	0.04	2.44	0.18	2.41	2.39	3.70	0.71	3.5	5.0	0.5			
SM-15 a2	0.11	1.82	0.05	2.33	0.12	2.42	0.39	3.70	0.66	12.2	18.4	2.1			e
SM-15 a3	0.04	2.92	0.04	2.60	0.17	2.41	0.82	3.70	0.64	3.7	5.8	0.7			
SM-15 a4	0.46	1.26	0.16	1.85	0.77	2.41	0.62	3.70	0.76	11.1	14.5	1.2			e
SM-15 a5	0.03	3.24	0.03	2.87	0.08	2.50	0.51	3.70	0.61	4.0	6.5	0.9			
SM-15 a6	0.08	2.13	0.07	2.16	0.17	2.42	2.56	3.70	0.69	4.8	7.0	0.8	6.1	0.4	
SM-16 a1	0.27	1.33	0.09	1.96	0.09	2.43	3.15	3.70	0.71	16.6	23.5	2.3			
SM-16 a2	0.90	1.01	0.36	1.82	0.28	2.41	1.98	3.70	0.73	16.9	23.2	2.1			
SM-16 a3	0.25	1.56	0.12	1.87	0.18	2.41	0.37	3.70	0.72	12.5	17.3	1.6			e
SM-16 a4	0.01	6.40	0.01	7.86	0.06	2.46	0.28	3.70	0.75	3.3	4.3	0.7			e
SM-16 a5	0.14	1.77	0.18	1.84	0.03	2.52	1.03	3.70	0.76	6.0	7.9	0.7			
SM-16 a7	0.04	3.25	0.09	1.90	0.07	2.44	0.55	3.70	0.69	3.1	4.4	0.5			e

[a] The amount of helium is given in nano-cubic-centimeters in standard temperature and pressure.
[b] Ejection correction (Ft): correction factor for α ejection (Farley et al., 1996; Hourigan et al., 2005).
[c] Uncertainty of the single-grain age is given as 2σ in percent (or in millions of years), and it includes both the analytical uncertainty and the estimated uncertainty of the Ft.
[d] Average ages for totally reset samples were calculated as the unweighted arithmetic mean.
[g] Uncertainty of the sample average age is 2 standard error as $(SD)/(n)1/2$, where SD is standard deviation of the age replicates and n is the number of age determinations.
[f] Ages with a substantial first He re-extract (> 4 %) and/or a total analytical error of > 10 % have been excluded. Outliers on the [He]−P plot have also been excluded (Vermeesch, 2008).

Miocene cumulative amount of shortening in the Subalpine Molasse and the Jura FTB decreases from the west to the east from ca. 30 km near Geneva to ca. 20 km near Lake Constance before decreasing to < 1 km between ca. 10.5° E and Salzburg (12.8° E; Fig. 6b).

5 Discussion

5.1 Uncertainty of the thermochronological data

Interpreting thermochronological ages from sedimentary basins may be challenging, as they potentially have been influenced by factors that are difficult to quantify. For instance, heat flux within the basin may have been variable through time when hydrothermal fluids may have heated or cooled the grains after deposition (Louis et al., 2019), or individual grains dated have different provenance histories that change their respective temperature sensitivity (Luijendijk, 2019). These uncertainties can result in a spread of single-grain ages within individual samples or along-strike the orogen, which cannot be explained by factors such as effective uranium content (e.g. Flowers et al., 2009) or broken grains (Brown et al., 2013). Provenance age is a particular problem for the interpretation of samples which have not been reset because, commonly, only three to five single-grain ages are reported, which makes statistical analysis of the grain age distributions difficult.

In our data set, we report two samples that show unreset ages (samples SM-7 and SM-16). These samples can only be used to infer a maximum amount of cooling of less than 60 °C. Interpreting the single-grain ages either as detrital ages or partially reset ages and deriving t–T histories for exhumation of the hinterland would require additional data. For completely reset samples, the provenance history of the single-grain ages is erased (Luijendijk, 2019). Single-grain ages of all other samples in our data set (SM-1, SM-4, SM-5, SM-6, SM-8, SM-11, SM-12, SM-13, SM-14, and SM-15) may be influenced by heat flux variations. Paleo-heat flux is notoriously difficult to constrain (Louis et al., 2019). However, as shown from a compilation of geothermal springs within the Alps, heat flux variations are spatially localized (Luijendijk et al., 2020). Consequently, this should be reflected in local outliers within the data set, for instance a suite of very young ages within a region. As our data are consistent with other data along-strike the Subalpine Molasse as far east as Lake Constance (von Hagke et al., 2012, 2014b), we consider local paleo-heat flux variations to be negligible and infer that the data reflect cooling associated with thrusting in the Subalpine Molasse.

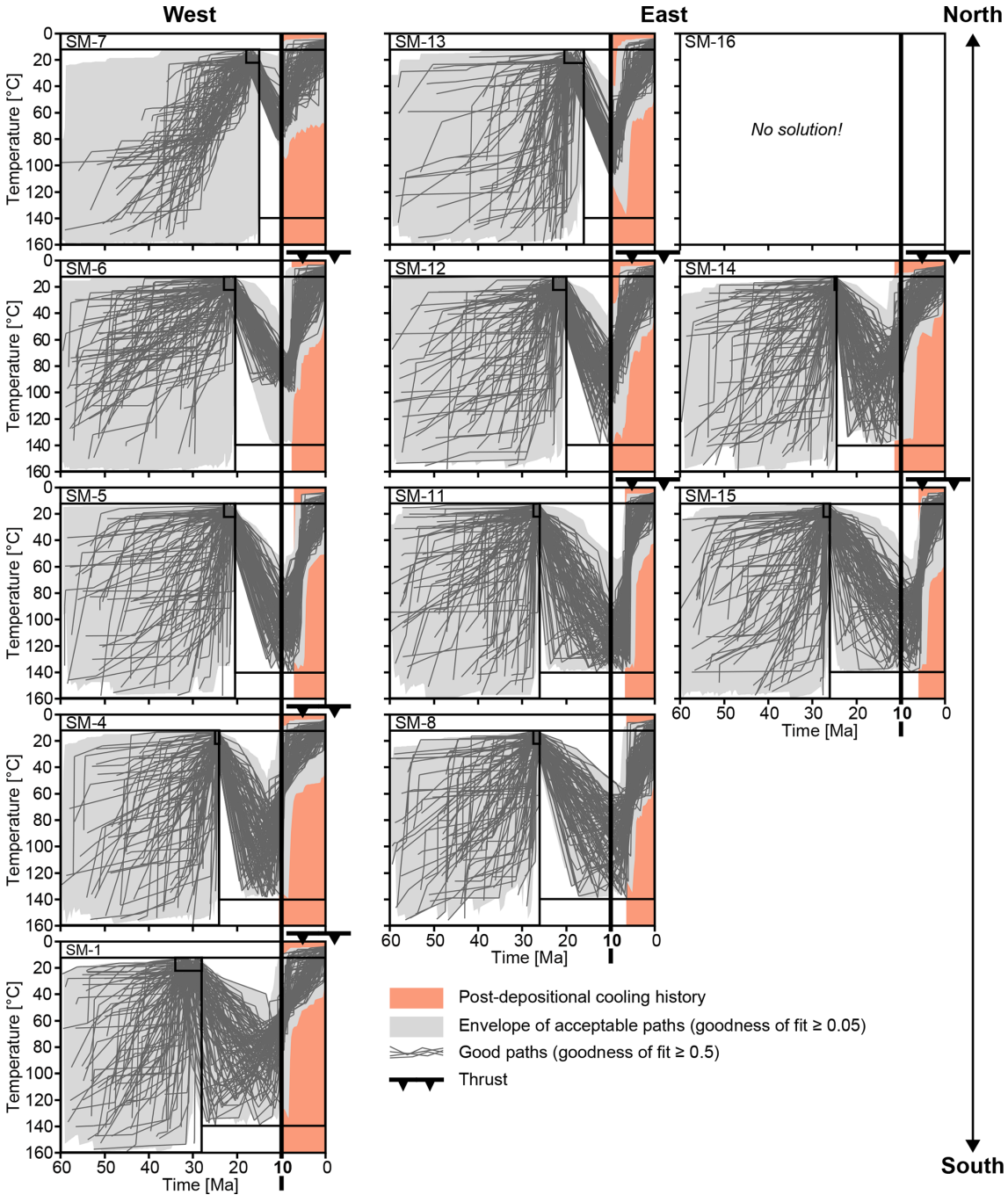

Figure 4. Thermal evolution of samples. The results from inverse modeling of apatite (U−Th−Sm)/He (AHe) ages with the HeFTy software (Ketcham, 2005) show the time–temperature history of the samples discussed in the text. Modeling constraints are shown as black boxes. The bold black lines at 10 Ma serve as a visual time reference. The thermal histories for the different samples are aligned from north to south and from east to west according to their sample location.

5.2 Local-scale stratigraphic architecture conditioning the pattern of strain accommodation

In the sampling area, mapping discloses along-strike differences in the litho-tectonic architecture of the Subalpine Molasse (Fig. 3). The sediments are thrust northwestward along SW–NE-striking thrusts. East of the Aar valley, a backthrust emerges at the surface and forms a frontal triangle zone (Figs. 3 and 5), a structure which is also known from parts of the Subalpine Molasse farther east (Fig. 7; e.g. Berge and Veal, 2005; von Hagke and Malz, 2018; Müller et al., 1988; Ortner et al., 2015; Schuller et al., 2015; Sommaruga et

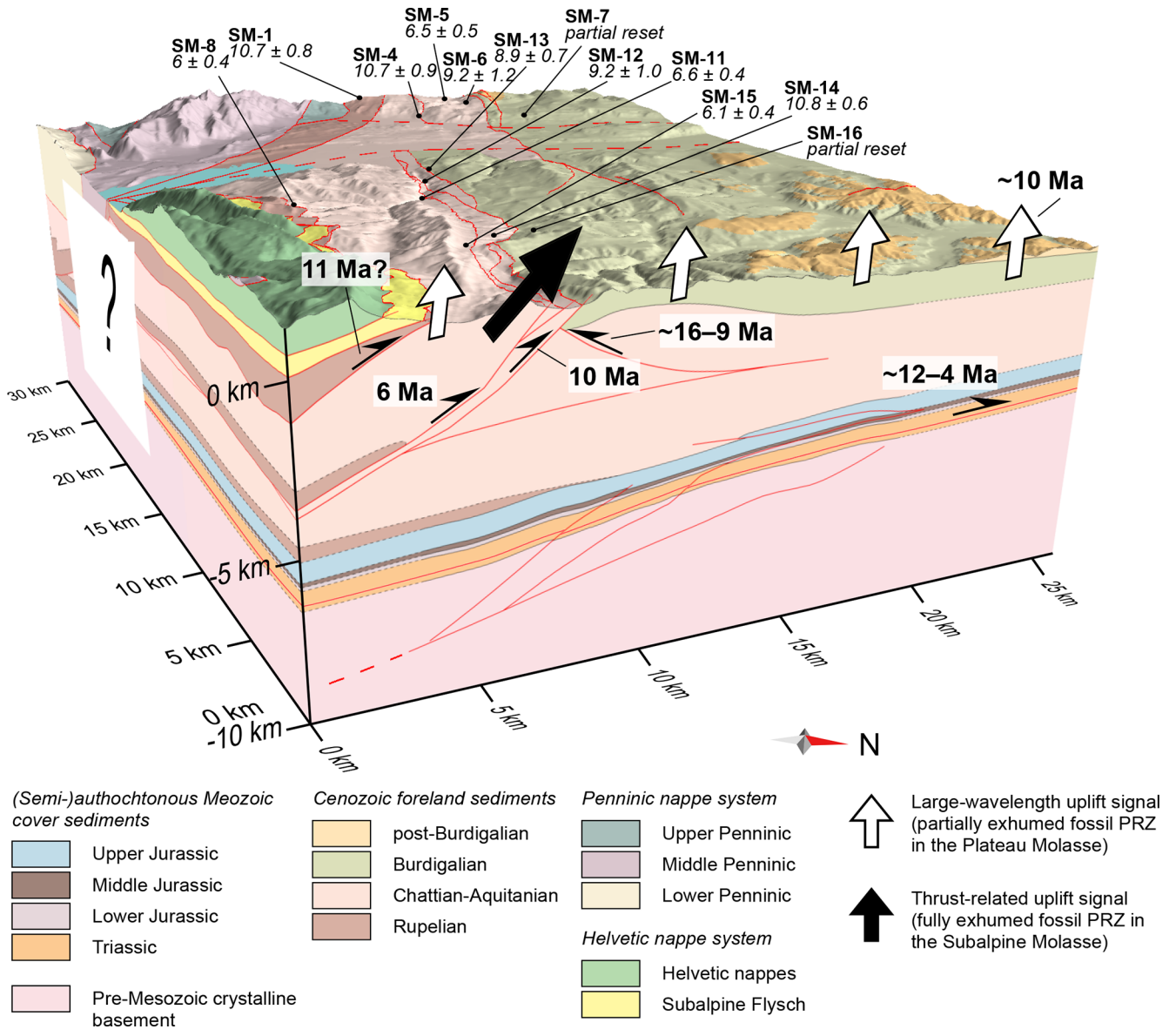

Figure 5. Block model of with sample locations and corresponding average (U−Th−Sm)/He ages. The construction of the block model is based on surface (Beck, 1945; Haus, 1937; Jordi, 2012; Rutsch, 1947; Schlunegger et al., 1993, 1997) and subsurface (2D seismic interpretation; Mock and Herwegh, 2017) geological information. PRZ, partial retention zone.

al., 2012; Stäuble and Pfiffner, 1991). The Aar valley, running across the study area, is characterized by a low relief and is filled by > 100 m thick Quaternary deposits (Fig. 5; Dürst Stucki et al., 2010). Accordingly, the structural configuration of this part of the study area is only poorly resolved. However, the structures of the Subalpine Molasse change abruptly across the Aar valley (Figs. 3 and 5), as has been described by many authors (Beck, 1945; Blau, 1966; Haus, 1937; Pfiffner, 2011; Rutsch, 1947; Vollmayr, 1992). Based on this observation and under the consideration of available interpreted reflection seismic lines, the presence of a possible syn-thrusting strike-slip fault zone running along the valley axis has been proposed (Mock and Herwegh, 2017; Pfiffner, 2011; Vollmayr, 1992). The presence of such a fault is, however, speculative due to the low resolution of the seismic data. The latter stems from (i) the thick Quaternary cover resulting in a very poor signal-to-noise ratio and (ii) the poorly resolved molasse strata as a result of the frequency, which was chosen in order to optimize for the targeted Mesozoic horizons below (Mock and Herwegh, 2017). An alternative explanation for the sudden along-strike change in the tectonic architecture has first been proposed by Rutsch (1947). He reported that the change from a mainly conglomeratic (east) to a sand- and mudstone-dominated (west) lithofacies coincides

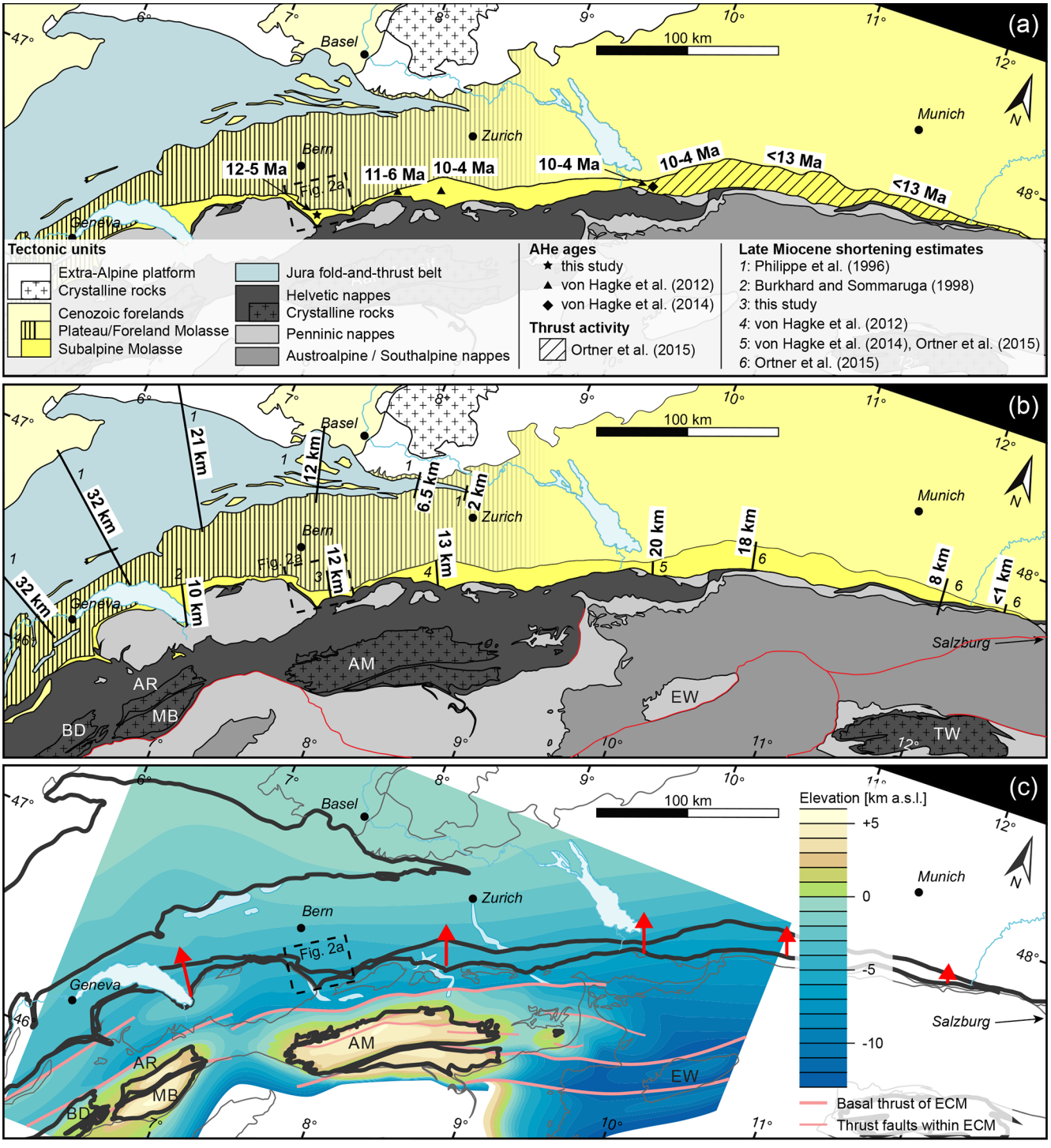

Figure 6. Along-strike variations in late-Miocene deformation of the north Alpine foreland between Lake Geneva and Salzburg. **(a)** Tectonic map (modified from Schmid et al., 2004) and activity of thrusting in the Subalpine Molasse deduced from AHe ages and geological interpretation. **(b)** Tectonic map (modified from Schmid et al., 2004) and estimated amount of late-Miocene shortening in the north Alpine foreland (i.e. Subalpine Molasse and Jura FTB). Estimates from the Subalpine Molasse record minimum shortening. **(c)** Top basement map of the Central Alps (modified from Pfiffner, 2011) showing the highly non-cylindrical hinterland architecture with the high-relief domains of the external crystalline massifs (ECMs). Red arrows indicate the constant late-Miocene deformation signal with a decrease in horizontal shortening recorded in the north Alpine foreland. AM, Aar Massif; AR, Aiguilles Rouges Massif; BD, Belledonne Massif; EW, Engadine Window; MB, Mont Blanc Massif; TW, Tauern Window.

with an increase in the folding intensity along the frontmost anticline (Falkenfluh anticline; Fig. 3a). Indeed, while conglomerates are the dominant lithofacies in the eastern part of the study area, they are vastly absent west of the Aar valley, where mainly alternating sequences of sandstones and mudstones outcrop (Figs. 3 and 7; Landesgeologie, 2005). This difference in mechanical stratigraphy east and west of the Aar valley is probably a result of an asymmetric dispersal system with a distinct northeastward direction of sediment discharge (Schlunegger and Norton, 2015). The distribution of mechanically different lithologies seems to control the pattern of thrusting. While east of the Aar valley, the mechanically stronger thick conglomeratic sequences deform en bloc (i.e. as one unit) and thrusts are concentrated in narrow bands following mechanically weak zones of sand- and mudstones, strain is accommodated in a much more distributed pattern along more closely spaced thrusts in the western part of the study area (Fig. 3). With deformation localizing along the pronounced mechanical contrast between conglomerates and sand- or mudstones, the large tectonic slice made up of amalgamated conglomerates east of the Aar valley is thrust northwestward en bloc. This is also manifested in well-defined and constant AHe ages of ca. 6 Ma within this tectonic slice (samples SM-8, SM-11, and SM-15; Figs. 3 and 5).

The observation that along-strike variations in the stratigraphic architecture lead to complex patterns of strain accommodation is not unique to our study area but can be also made at the Mont Pèlerin, the Rigi, or the Hörnli in western, central, and eastern Switzerland, respectively (Fig. 7). Salients seem to occur at the apex of former alluvial megafan depositional systems, while recesses are observed in regions in between these large dispersal systems, where thick conglomerate sequences are missing. The lithological control on the strain accommodation and exhumation pattern is particularly well observed in the Rigi area (profile 3 in Fig. 7; Sommaruga et al., 2012). The thick conglomerate sequence of the Rigi thrust sheet was (re-)activated en bloc at ca. 5 Ma, while the adjacent sand- and mudstone-dominated part to the north experienced a period of thrusting at ca. 9 Ma along evenly spaced faults (von Hagke et al., 2012). Similar dependencies between the style of deformation and lateral changes in lithology have also been described for the Subalpine Molasse in Bavaria and western Austria (for detailed information, see Ortner et al., 2015), as well as for the basal detachments of the Subalpine Molasse and the Jura FTB (von Hagke et al., 2014a). While large alluvial fans formed thick conglomerate-sandstone sequences in western Bavaria, brackish to shallow marine conditions prevailed farther east where marls and sandstones were deposited (Frisch et al., 1998; Kuhlemann and Kempf, 2002). This lateral change in the molasse's mechanical stratigraphy has been described as having a direct influence on the deformation style of the Subalpine Molasse (Ortner et al., 2015). While stacks of tectonic horse structures and a pronounced triangle zone developed in western Bavaria, the deformation style changes to buckle folding farther east, which decreases in amplitude and the triangle zone disappears (a detailed description is provided in Ortner et al., 2015). Numerical models of syntectonic sedimentation support the idea that sediments shed on an evolving FTB strongly control its geometry and may include the formation of backthrusts (e.g. Fillon et al., 2013).

5.3 Implications for late orogenic processes

5.3.1 The link to exhumation of the external crystalline massifs

Classically, thrusting in the Jura FTB and the Subalpine Molasse between Lake Geneva and Lake Constance has been kinematically and spatiotemporally related to the uplift and exhumation of the ECMs and to the propagation of the deformation front towards the foreland (Burkhard, 1990; Burkhard and Sommaruga, 1998; Pfiffner et al., 1997). Note that according to Campani et al. (2012), von Hagke et al. (2014b), and Schlunegger and Kissling (2015), the mean elevation of the Alpine topography has not changed since the early Miocene, and we can assume steady-state conditions between rock uplift and surface erosion for this time interval. In this case, we can consider rock uplift and exhumation rates to be similar. The Aar, and possibly also the Mont Blanc, and Aiguilles Rouges massifs were exhumed in early to mid-Miocene times during a stage of differential rock uplift along subvertical reverse faults (vertical tectonics; Herwegh et al., 2017, 2020). This stage of vertical tectonics was followed by late-Miocene en bloc rock uplift and exhumation above a series of shallow southwest-dipping basal thrusts at the massif's northwestern front (Egli et al., 2017; Herwegh et al., 2017, 2020). It is during this late (ca. post-13 Ma) thrusting-dominated stage (i.e. horizontal tectonics) that deformation was translated northward into the Alpine foreland. In the non-detached part of the north Alpine foreland, thrusting of the proximal molasse occurred. In the western north Alpine foreland, large-scale strain partitioning occurred when deformation propagated 50—90 km to the north forming the Jura FTB, while at the same time imbricates of Subalpine Molasse were thrust northward (e.g. Becker, 2000; Burkhard, 1990; Burkhard and Sommaruga, 1998; von Hagke et al., 2012).

However, it has also been reported that the proximal foreland basin east of the easternmost ECM, i.e. the Aar Massif, has been subject to post-12 Ma thrusting and horizontal shortening (Fig. 6a and b; Ortner et al., 2015). Our AHe age data from the Subalpine Molasse (Figs. 3, 4, and 5) fit with AHe ages farther east (von Hagke et al., 2012, 2014b) and chronicle a period of thrusting and exhumation of the Subalpine Molasse between 12 and 4 Ma (Fig. 6a). This occurred coevally with the main deformation phase in the Jura FTB, which lasted from ca. 12 to 4 Ma (e.g. Becker, 2000). Similar ages constrained from geological and seismic interpretation, and observations of growth strata in the youngest

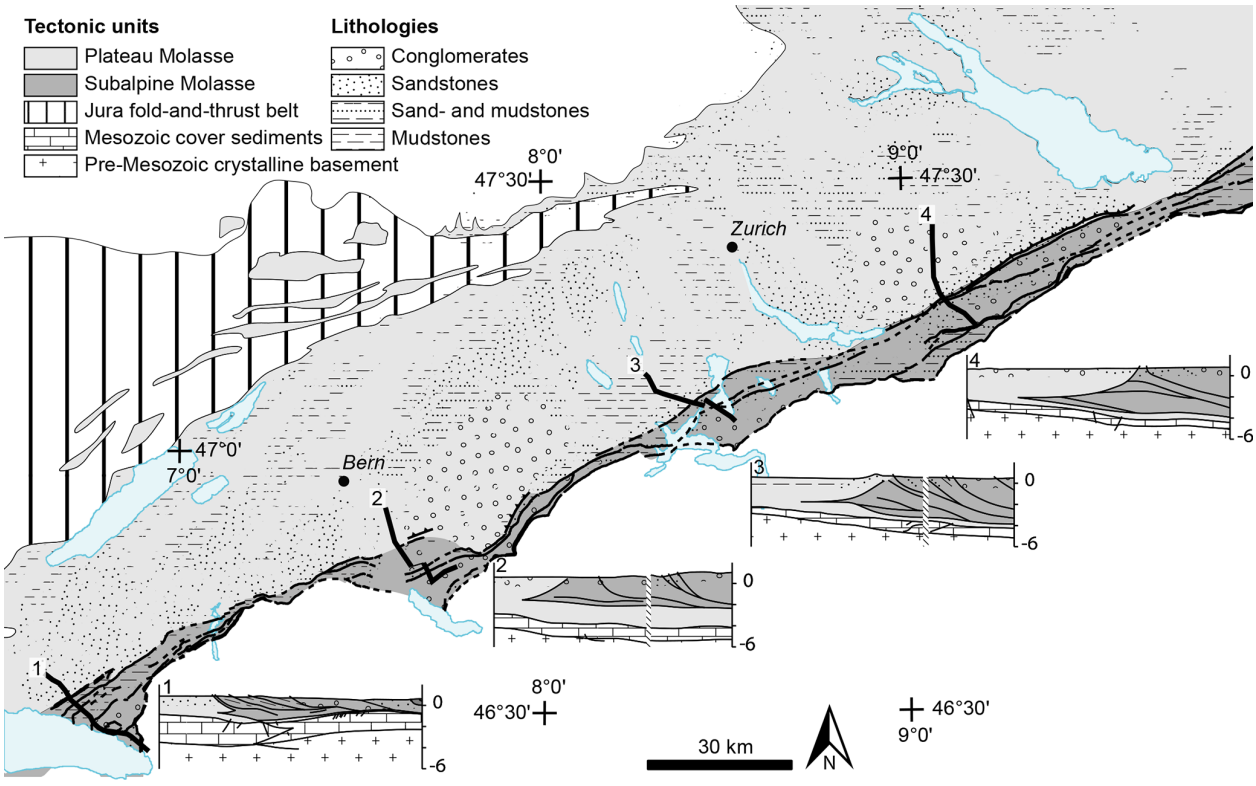

Figure 7. Litho-tectonic map of the Swiss Molasse Basin (modified from Landesgeologie, 2005). Cross sections 1–4 are based on 2D seismic interpretation (cross section 2 – Mock and Herwegh, 2017; cross sections 1, 3, and 4, Sommaruga et al., 2012).

preserved sediments have been reported for the Subalpine Molasse between Lake Constance and Salzburg (Fig. 6a; Ortner et al., 2015). Late-Miocene thrusting in the Subalpine Molasse of Central Switzerland has also been inferred from stratigraphic data (Haus, 1935). Since the youngest AHe ages are recorded from the internal tectonic slices of the Subalpine Molasse (Figs. 3, 4, and 5), we can infer the occurrence of break-back thrusting (i.e. back-stepping sequence of thrusting), a characteristic feature, which has been confirmed so far along the Subalpine Molasse between Bern and Salzburg based on thermochronological data and cross section restorations (von Hagke et al., 2012, 2014b; Ortner et al., 2015; Schuller et al., 2015) but has been locally argued for as early as the 1930s (Haus, 1935, 1937). The break-back thrusts are supposedly younger than the development of the frontal triangle zone, which formed the active northern deformation front from ca. 20 to 12 Ma (von Hagke et al., 2014b; Ortner et al., 2015). Furthermore, our AHe ages from the Plateau Molasse record a partially exhumed PRZ (Figs. 3, 4, and 5) and thus corroborate the occurrence of substantial exhumation of the flat-lying Plateau and Foreland Molasse (Cederbom et al., 2011; Genser et al., 2007; Gusterhuber et al., 2012; von Hagke et al., 2012; Zweigel et al., 1998), indicating a large-scale exhumation signal across the entire basin.

Although foreland deformation is kinematically linked to the late stage of thrust-dominated exhumation of the ECMs (horizontal tectonics; Herwegh et al., 2017, 2020), the occurrence of late-Miocene thrusting in the foreland is not restricted to the areas in front of the ECMs. This can be observed east of the Aar Massif, where the basement topography in the hinterland decreases rapidly towards the east (Fig. 6c), while horizontal shortening within the foreland remains constant at ca. 20–18 km (Fig. 6b). Furthermore, we observe that short-wavelength along-strike variations in the hinterland's basement topography, i.e. the different levels of exhumed basement blocks, are not reflected in the observed amounts of horizontal shortening within the foreland. However, looking at the pattern over a longer wavelength (ca. 500 km, i.e. the length of the northern Central Alps), the general disappearance of the ECMs towards the east and the decrease in foreland shortening are in good correlation (Fig. 6). Combining these observations with the aforementioned data about the timing and kinematics of ECM exhumation and foreland deformation, we suggest that late-Miocene thrusting is a long-wavelength feature which occurs along the entire northern Central Alps, encompassing both the ECMs and the foreland (i.e. Subalpine Molasse and Jura FTB; Fig. 8c). Along the western portion of the Central Alps, this follows an early to mid-Miocene stage, which was characterized by the subvertical extrusion of the eastern ECMs and a stationary deformation front in the Subalpine Molasse. Hence, along the northern front of the western Central Alps, the mid–

late-Miocene boundary marks the transition from an inferred buoyancy-driven regime with the subvertical rise of the eastern ECMs (vertical tectonics; Herwegh et al., 2017, 2020) to a large-scale thrust-dominated regime (horizontal tectonics) encompassing also the northern front of the eastern Central Alps (i.e. east of the ECMs) thereafter.

5.3.2 Possible link to geodynamic processes beneath the core of the Central Alps

After the early stages of post-35 Ma continent–continent collision, plate convergence rates seemed to decrease noticeably at ca. 20 Ma (Fig. 8b; Handy et al., 2010; Schmid et al., 1996). At this stage, pro-wedge widening of the Molasse Basin came to a relative halt (Fig. 8a). In the Central Alps, the proximal part of the basin kept subsiding by an additional 2–3 km (Burkhard and Sommaruga, 1998; Schlunegger and Kissling, 2015), while the distal realm became subject to erosion (Kuhlemann and Kempf, 2002). This phase was also associated with the period of differential vertical uplift of the Aar Massif (and probably also the Mont Blanc and Aiguilles Rouges massifs), i.e. its rise along steeply dipping reverse shear zones between ca. 20 and 12 Ma (Herwegh et al., 2017, 2020; Wehrens et al., 2017), while the northern deformation front remained stationary in the Subalpine Molasse (Fig. 8c; Burkhard and Sommaruga, 1998; von Hagke et al., 2014b; Ortner et al., 2015). East of Munich, however, the Molasse Basin experienced, at this time, a period of uniform subsidence and even a short-lived phase of uplift (ca. 17–16 Ma) as evidenced by horizontal to 5° westward tilting strata of post 20 Ma molasse sediments (Gusterhuber et al., 2012; Zweigel et al., 1998). The latter was attributed to eastward-directed lateral extrusion of crustal blocks (Gusterhuber et al., 2012). It also correlates with the observed westward increasing gradient of crustal thickening associated with an eastward decrease in the mean elevation of the Eastern Alps (Rosenberg et al., 2018). Alternatively, Handy et al. (2015) explained this signal as a result of deep crustal unloading due to a proposed slab tear and a corresponding subduction polarity reversal beneath the Eastern Alps, which has been proposed to have occurred at ca. 20 Ma (Handy et al., 2015; Schmid et al., 2013; Ustaszewski et al., 2008). These observations imply that important along-strike changes and a large-scale geodynamic (Hetényi et al., 2018b; Kissling et al., 2006; Lippitsch et al., 2003; Mitterbauer et al., 2011) and tectonic (e.g. Handy et al., 2015; Ratschbacher et al., 1991; Rosenberg et al., 2018) decoupling between the Central and the Eastern Alps and their Molasse Basins were established in Miocene times. We suggest that this is also mirrored by the along-strike pattern in late-Miocene cumulative horizontal shortening in the north Alpine foreland, which, without fully considering the possibly large uncertainties of shortening estimation in the Subalpine Molasse, seems to decrease from ca. 30 km near Lake Geneva to ca. 20 km near Lake Constance. A decrease from ca. 18 to < 1 km is finally recorded east of ca. 10.5° E (Fig. 6). East of Salzburg at the front of the Eastern Alps, zero late-Miocene shortening is recorded in the proximal molasse (Beidinger and Decker, 2014; Hinsch, 2013; Ortner et al., 2015). This pattern has been attributed to an increasing transfer of shortening towards the internal parts of the orogen (i.e. the Tauern Window) and to the out-of-section removal of crust through lateral extrusion in the Eastern Alps (Ortner et al., 2006, 2015). While such upper-crustal processes may certainly mask the signal of late-Miocene foreland deformation, the latter may also reflect the response to the change in a geodynamic driving force operating at a larger scale, situated at deeper crustal levels, and encompassing the entire Central Alps (Fig. 9).

In the context of the aforementioned observations, we propose that the attached European lithospheric slab beneath the Central Alps presents a possible candidate for driving the inferred long-wavelength signal of late-Miocene foreland deformation (Fig. 9). This hypothesis is based on the following main observations and considerations. (i) The along-strike extent of late-Miocene thrusting in the foreland correlates remarkably well spatially with the proposed extent of the steeply south-dipping Central Alpine European slab imaged by seismic tomography (Fig. 9; Kästle et al., 2020; Lippitsch et al., 2003; Zhao et al., 2016). (ii) The long spatial wavelength of tectonically driven exhumation of the Subalpine Molasse, which has been attributed to distinct thrusting events between ca. 12 and 4 Ma, can be viewed as an upper-crustal expression of a lithospheric-scale tectonic driver acting at that wavelength. (iii) The segmentation of the deep structure of the Central and Eastern Alps (Hetényi et al., 2018b; Kästle et al., 2020; Kissling et al., 2006; Lippitsch et al., 2003; Mitterbauer et al., 2011) has been conjectured to have occurred at ca. 20 Ma and induced a geodynamic and tectonic reorganization along the Alpine chain thereafter (Handy et al., 2015; Schmid et al., 2013; Ustaszewski et al., 2008). Hence, this time constraint allows us to discuss the Central Alpine late-Miocene foreland deformation (which is decoupled from the Eastern Alps) in the context of the ongoing evolution of the segmented Central Alpine slab. The corresponding transition in the macro-tectonic regime of the northern Central Alps from inferred buoyancy-driven vertical to large-scale horizontal tectonics may reflect the response to the decreasing rates of European slab rollback and a late phase of post-collisional indentation of the Adriatic plate as recently proposed by Herwegh et al. (2017, 2020).

5.3.3 The exceptional position of the Bavarian Subalpine Molasse

The configuration of the lithospheric mantle slabs is inherently different beneath the Central and the Eastern Alps (Kästle et al., 2020; Kissling et al., 2006; Kissling and Schlunegger, 2018; Lippitsch et al., 2003; Mitterbauer et al., 2011; Zhao et al., 2016). At the lithospheric scale, a polarity reversal between the European slab and the Adriatic slab has been

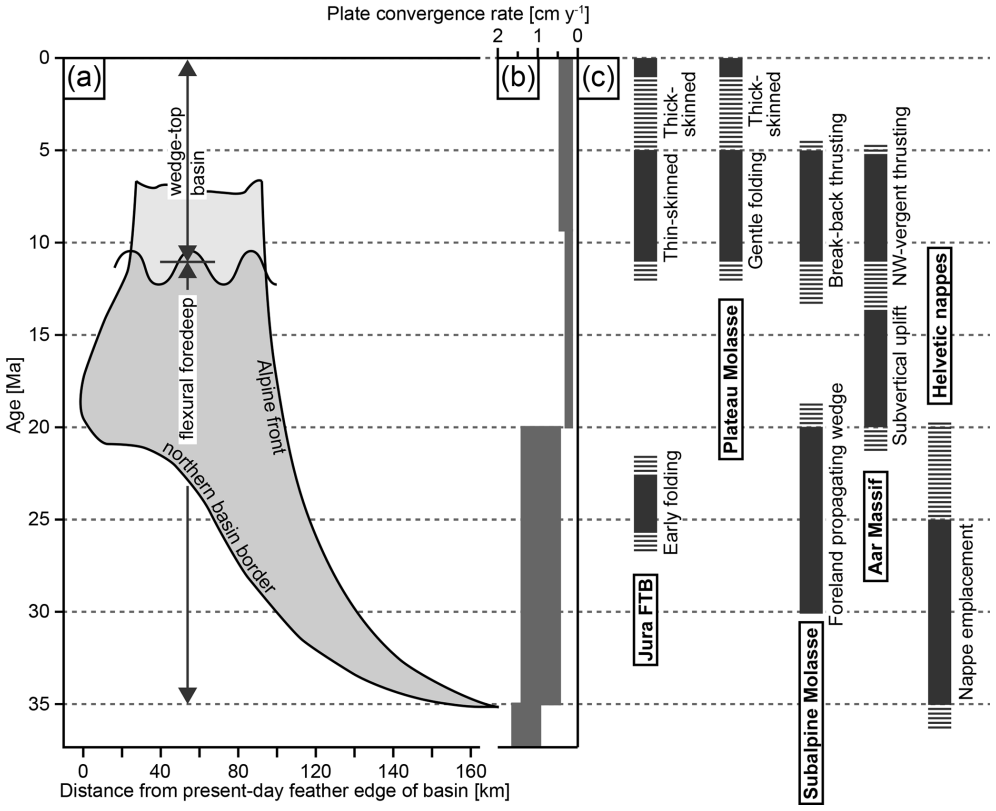

Figure 8. Oligocene to present-day evolution of the northern Central Alps. **(a)** Temporal evolution of the Molasse Basin architecture (adapted from Schlunegger and Kissling, 2015). The location of the section is given in Fig. 1. **(b)** Rates of plate convergence between the Adriatic plate and Europe (Handy et al., 2010; Schmid et al., 1996). **(c)** Tectonic evolution of the major tectonic units of the northern Central Alps. FTB, fold-and-thrust belt.

conjectured beneath the western Tauern Window (Lippitsch et al., 2003). However, this model is currently debated as new geophysical data indicate that at depth the southward-dipping European slab extends from the Central Alps until east of the Giudicarie and Brenner Faults (Kästle et al., 2020) and possibly as far east as the central Tauern Window (Figs. 1 and 9; Qorbani et al., 2015). Based on tomographic results from the AlpArray initiative, Hetényi et al. (2018b) propose that at ca. 13° E a northward-dipping slab of the Adriatic plate is present. All these studies show that the deep structure remains very uncertain and debated since tomographic data have been interpreted in different ways regarding the slab geometries at depth (Hetényi et al., 2018b; Kästle et al., 2020; Lippitsch et al., 2003; Mitterbauer et al., 2011; Zhao et al., 2016). However, they all concur on the observation that between the deep velocity anomalies of the Central and the Eastern Alps a major discontinuity is present east of the Giudicarie and Brenner Faults (see also Handy et al., 2015). This correlates with the eastward termination of the late-Miocene Subalpine Molasse near Salzburg (Fig. 9). We thus propose that the geophysical data place the link between the deep structure and deformation of the Subalpine Molasse between Lake Constance and Salzburg in a Central Alpine rather than an Eastern Alpine context.

While at the mantle scale, a segmentation of the slab structure is observed between ca. 11 and 13° E (Fig. 9), an along-strike segmentation at crustal levels occurs at the Brenner Fault. East of the Brenner Fault (Figs. 1 and 9), the post-collisional evolution of the Eastern Alps is characterized by the northward indentation of the Dolomite indenter and the related eastward lateral extrusion of crustal blocks (Ratschbacher et al., 1991). At the larger scale, this was possibly facilitated by slab retreat beneath the Carpathians and the associated rifting in the Pannonian Basin (Peresson and Decker, 1997). The main phase of lateral extrusion occurred in early and mid-Miocene times (Frisch et al., 1998; Ratschbacher et al., 1991), possibly extending into the late Miocene (Ortner et al., 2015). These processes were additionally associated with the collisional exhumation of the Tauern Window and normal faulting along its bounding low-angle normal faults (see Rosenberg et al., 2018). In this respect, the Bavarian Subalpine Molasse is particularly interesting, since it extends over this transition area (Fig. 9). We suggest that in this transient position, the tectonics of this segment of the Subalpine Molasse between Lake Constance

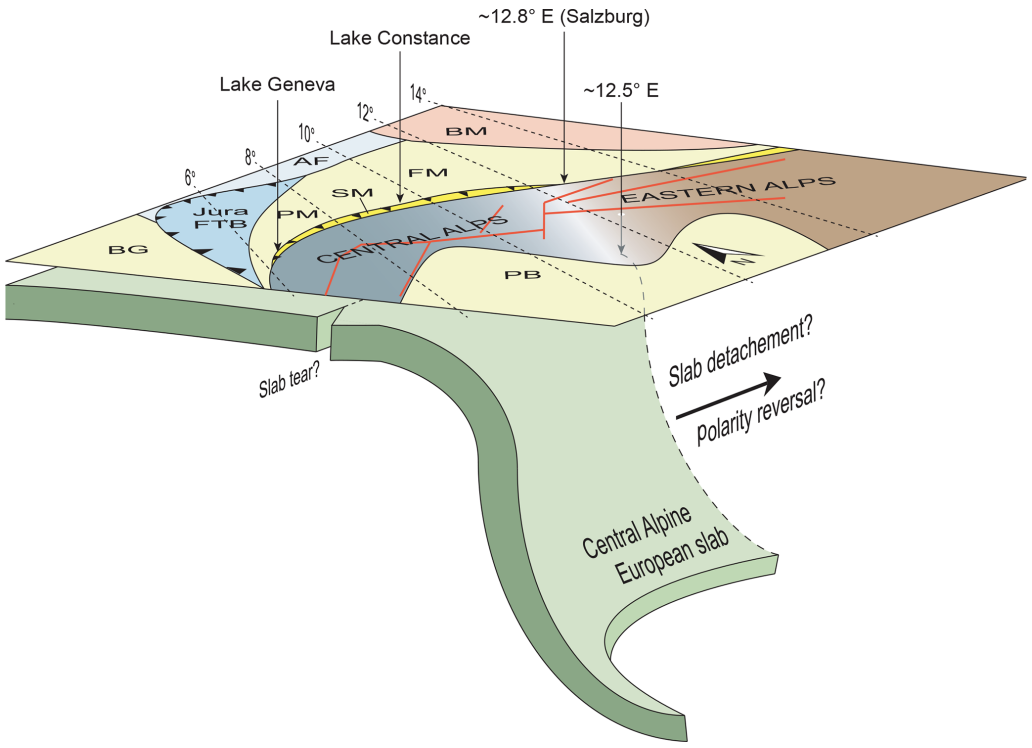

Figure 9. Schematic 3D representation of the structure of the Central Alpine European slab and its spatial correlation with the eastward termination of the late-Miocene Subalpine Molasse near Salzburg. PM, Plateau Molasse; FM, Foreland Molasse; SM, Subalpine Molasse; PB, Po Basin; TW, Tauern Window; BF, Brenner Fault; FTB, fold-and-thrust belt; BG, Bresse Graben; AF, autochthonous foreland; BM, Bohemian Massif.

and Salzburg was probably affected by the deep-seated dynamics of the Central Alpine European slab, while at the same time also being masked by the aforementioned upper-crustal processes of Eastern Alpine tectonics (e.g. lateral extrusion).

In order to resolve the influence of deep-seated processes on the tectonics of the Subalpine Molasse and the foreland basin in general, we propose that the present-day slab geometries underneath the entire Alps must be resolved at higher resolution. Furthermore, the time evolution of the slabs must be constrained with a focus on if, when, and how a potential subduction polarity reversal occurred in the Eastern Alps. These studies should be supported by source-to-sink analyses linking the stratigraphy of the foreland to hinterland processes. New thermochronological data from the Bavarian Subalpine and Foreland (i.e. undeformed) Molasse will be essential. Furthermore, we expect that ongoing seismotomographic investigations will disclose further details to constrain the deep-seated driving mechanisms (Hetényi et al., 2018a).

6 Conclusions

In this paper, we presented new low-temperature thermochronological age data from the Subalpine Molasse of the Central European Alps. By comparing our results to published age and stratigraphic data along-strike the Alps from Lake Geneva to Salzburg we conclude the following.

- (U−Th−Sm)/He ages along the Subalpine Molasse of the Central Alps record thrust-related exhumation between 12 and 4 Ma with at least two thrusting pulses associated with it at ca. 10 and 6 Ma.

- The pattern of strain accommodation is strongly conditioned by the local-scale mechanical stratigraphy, since the locus of deformation depends on the distribution of mechanically weak (sand- and mudstone) and strong (conglomerate) lithologies. Accordingly, a general widening of the foreland thrust belt (i.e. tectonic salients) and en bloc deformation of large conglomerate bodies occurs at the locations where the lithology is conglomerate dominated, i.e. at the site of former megafan dispersal systems depositing large and kilometer-thick conglomerate sequences into the foreland. Conversely, tectonic recesses and a more distributed deformation pattern developed where the mechanical stratigraphy is dominated by sand- and mudstone deposits.

Hence, we observe that the deformation style during late-Miocene thrusting of the Subalpine Molasse is masked by

local variations in the stratigraphic architecture. However, in terms of timing and kinematics, thrust-related shortening, though decreasing in intensity from the west to the east, is consistent along-strike in those parts of the Alps which correlate with the lateral (i.e. along-strike) extent of the Central Alpine lithospheric mantle slab at depth. Thus, we may interpret late-Miocene long-wavelength thrusting as an upper-crustal signal resulting from this lithospheric driving force. The latter possibly leads to a change in the macro-tectonic regime in the western Central Alps at ca. 12 Ma, from vertical to thrusting-dominated horizontal tectonics.

Finally, although we lack the required data to precisely determine the geodynamic processes responsible for the late phase of shortening in the molasse, we are able to constrain the timing of this event to 12–4 Ma. In addition, this work shows that low-temperature thermochronological data yield an improved understanding of the chronology of orogenic processes where the late orogenic stage of a mountain belt may be characterized by a complex pattern of strain release conditioned by site-specific stratigraphic and thus lithological conditions at the local scale and by widespread tectonism possibly resulting from changes in deep-seated driving forces.

Data availability. The research data are included in this paper and in the Supplement and can be freely accessed.

Supplement. The supplement related to this article is available online at: https://doi.org/10.5194/se-11-1823-2020-supplement.

Author contributions. SM designed the study with support from MH, FS, and CvH. FS and MH assisted SM during sampling in the field. SM carried out mineral separation and picked the apatite crystals. ID carried out the helium extraction and the ICP-MS measurements at the University of Göttingen. CvH and ID assisted in analyzing and interpreting the apatite (U−Th−Sm)/He ages. SM prepared the paper, with contributions from all co-authors.

Competing interests. The authors declare that they have no conflict of interest.

Acknowledgements. We thank Judith Dunkl (Göttingen) for assisting in the selection of apatite crystals, Pierre Valla (Bern) for discussions on the AHe ages and the thermal models, and Edi Kissling (Zurich) for his insights on lithospheric-scale processes. The paper has greatly benefited from detailed and constructive comments by Claudio Rosenberg (Paris), Giovanni Luca Cardello (Rome) Hugo Ortner (Innsbruck), and Nicola Levi (Vienna). Additional information on the data can be found in the Supplement. The study was funded by the Swiss Geological Survey of the Federal Office of Topography (swisstopo) as part of the GeoMol CH project. We acknowledge the use of the Move Software Suite (used for Fig. 5) granted by Petroleum Experts Limited.

Review statement. This paper was edited by Susanne Buiter and reviewed by Claudio Rosenberg and Giovanni Luca Cardello.

References

Allen, P. A., Crampton, S. L., and Sinclair, H. D.: The inception and early evolution of the North Alpine Foreland Basin, Switzerland, Basin Res., 3, 143–163, https://doi.org/10.1111/j.1365-2117.1991.tb00124.x, 1991.

Aubert, D.: Sur l'existence d'une ride de plissement oligocène dans le Jura vaudois, Bull. la Société Neuchâteloise des Sci. Nat., 81, 47–54, 1958.

Bachmann, G. H. and Müller, M.: Sedimentary and structural evolution of the German Molasse Basin, Eclogae Geol. Helv., 85, 519–530, https://doi.org/10.5169/seals-167019, 1992.

Baran, R., Friedrich, A. M., and Schlunegger, F.: The late Miocene to Holocene erosion pattern of the Alpine foreland basin reflects Eurasian slab unloading beneath the western Alps rather than global climate change, Lithosphere, 6, 124–131, https://doi.org/10.1130/L307.1, 2014.

Beck, P.: Über den Mechanismus der subalpinen Molassetektonik, Eclogae Geol. Helv., 38, 353–368, 1945.

Becker, A.: The Jura Mountains – an active foreland fold-and-thrust belt?, Tectonophysics, 321, 381–406, https://doi.org/10.1016/S0040-1951(00)00089-5, 2000.

Beidinger, A. and Decker, K.: Quantifying Early Miocene in-sequence and out-of-sequence thrusting at the Alpine-Carpathian junction, Tectonics, 33, 222–252, https://doi.org/10.1002/2012TC003250, 2014.

Berge, T. B. and Veal, S. L.: Structure of the Alpine foreland, Tectonics, 24, TC5011, https://doi.org/10.1029/2003TC001588, 2005.

Berger, A., Wehrens, P., Lanari, P., Zwingmann, H., and Herwegh, M.: Microstructures, mineral chemistry and geochronology of white micas along a retrograde evolution: An example from the Aar massif (Central Alps, Switzerland), Tectonophysics, 721, 179–195, https://doi.org/10.1016/j.tecto.2017.09.019, 2017.

Blau, R. V.: Molasse und Flysch im östlichen Gurnigelgebiet (Kt. Bern), Beiträge zur Geol. Karte der Schweiz, Schweizerische Geologische Kommission, Bern, NF 125, 151 pp., 1966.

Boyer, S. E. and Elliott, D.: Thrust systems, Am. Assoc. Pet. Geol. Bull., 66, 1196–1230, 1982.

Brown, R. W., Beucher, R., Roper, S., Persano, C., Stuart, F., and Fitzgerald, P.: Natural age dispersion arising from the analysis of broken crystals. Part I: Theoretical basis and implications for the apatite (U–Th)/He thermochronometer, Geochim. Cosmochim. Ac., 122, 478–497, https://doi.org/10.1016/j.gca.2013.05.041, 2013.

Burkhard, M.: Aspects of the large-scale Miocene deformation in the most external part of the Swiss Alps (Subalpine Molasse to Jura fold belt), Eclogae Geol. Helv., 83, 559–583, 1990.

Burkhard, M. and Sommaruga, A.: Evolution of the western Swiss Molasse basin: structural relations with the Alps and

the Jura belt, Geol. Soc. London, Spec. Publ., 134, 279–298, https://doi.org/10.1144/GSL.SP.1998.134.01.13, 1998.

Buxtorf, A.: Prognosen und Befunde beim Hauensteinbasis- und Grenchenbergtunnel und die Bedeutung der letzteren für die Geologie des Juragebirges, Verhandlungen der Naturforschenden Gesesellschaft Basel, 27, 184–254, 1916.

Campani, M., Mulch, A., Kempf, O., Schlunegger, F., and Mancktelow, N.: Miocene paleotopography of the Central Alps, Earth Planet. Sci. Lett., 337–338, 174–185, https://doi.org/10.1016/j.epsl.2012.05.017, 2012.

Caputo, R., Poli, M. E., and Zanferrari, A.: Neogene–Quaternary tectonic stratigraphy of the eastern Southern Alps, NE Italy, J. Struct. Geol., 32, 1009–1027, https://doi.org/10.1016/j.jsg.2010.06.004, 2010.

Cardello, G. L., Di Vincenzo, G., Giorgetti, G., Zwingmann, H., and Mancktelow, N.: Initiation and development of the Pennine Basal Thrust (Swiss Alps): a structural and geochronological study of an exhumed megathrust, J. Struct. Geol., 126, 338–356, https://doi.org/10.1016/j.jsg.2019.06.014, 2019.

Castellarin, A. and Cantelli, L.: Neo-Alpine evolution of the Southern Eastern Alps, J. Geodyn., 30, 251–274, https://doi.org/10.1016/S0264-3707(99)00036-8, 2000.

Cederbom, C. E., Sinclair, H. D., Schlunegger, F., and Rahn, M. K.: Climate-induced rebound and exhumation of the European Alps, Geology, 32, 709–712, https://doi.org/10.1130/g20491.1, 2004.

Cederbom, C. E., van der Beek, P., Schlunegger, F., Sinclair, H. D., and Oncken, O.: Rapid extensive erosion of the North Alpine foreland basin at 5-4 Ma, Basin Res., 23, 528–550, https://doi.org/10.1111/j.1365-2117.2011.00501.x, 2011.

Champagnac, J.-D., Molnar, P., Anderson, R. S., Sue, C., and Delacou, B.: Quaternary erosion-induced isostatic rebound in the western Alps, Geology, 35, 195–198, https://doi.org/10.1130/G23053A.1, 2007.

Chemenda, A. I., Burg, J. P., and Mattauer, M.: Evolutionary model of the Himalaya-Tibet system: Geopoem based on new modelling, geological and geophysical data, Earth Planet. Sci. Lett., 174, 397–409, https://doi.org/10.1016/S0012-821X(99)00277-0, 2000.

Davies, J. H. and von Blanckenburg, F.: Slab breakoff: A model of lithosphere detachment and its test in the magmatism and deformation of collisional orogens, Earth Planet. Sci. Lett., 129, 85–102, https://doi.org/10.1016/0012-821X(94)00237-S, 1995.

DeCelles, P. G. and Giles, K. A.: Foreland basin systems, Basin Res., 8, 105–123, https://doi.org/10.1046/j.1365-2117.1996.01491.x, 1996.

Dürst Stucki, M., Reber, R., and Schlunegger, F.: Subglacial tunnel valleys in the Alpine foreland: an example from Bern, Switzerland, Swiss J. Geosci., 103, 363–374, https://doi.org/10.1007/s00015-010-0042-0, 2010.

Egli, D., Mancktelow, N., and Spikings, R.: Constraints from $^{40}Ar/^{39}Ar$ geochronology on the timing of Alpine shear zones in the Mont Blanc-Aiguilles Rouges region of the European Alps, Tectonics, 36, 730–748, https://doi.org/10.1002/2016TC004450, 2017.

Farley, K. A.: (U-Th)/He Dating: Techniques, Calibrations, and Applications, Rev. Mineral. Geochemistry, 47, 819–844, https://doi.org/10.2138/rmg.2002.47.18, 2002.

Farley, K. A., Wolf, R. A., and Silver, L. T.: The effects of long alpha-stopping distances on (U-Th)/He ages, Geochim. Cosmochim. Ac., 60, 4223–4229, https://doi.org/10.1016/S0016-7037(96)00193-7, 1996.

Fillon, C., Huismans, R. S., and van der Beek, P.: Syntectonic sedimentation effects on the growth of fold-and-thrust belts, Geology, 41, 83–86, https://doi.org/10.1130/G33531.1, 2013.

Flowers, R. M., Ketcham, R. A., Shuster, D. L., and Farley, K. A.: Apatite (U–Th)/He thermochronometry using a radiation damage accumulation and annealing model, Geochim. Cosmochim. Ac., 73, 2347–2365, https://doi.org/10.1016/j.gca.2009.01.015, 2009.

Fox, M., Herman, F., Willett, S. D., and Schmid, S. M.: The Exhumation history of the European Alps inferred from linear inversion of thermochronometric data, Am. J. Sci., 316, 505–541, https://doi.org/10.2475/06.2016.01, 2016.

Frisch, W., Kuhlemann, J., Dunkl, I., and Brügel, A.: Palinspastic reconstruction and topographic evolution of the Eastern Alps during late Tertiary tectonic extrusion, Tectonophysics, 297, 1–15, https://doi.org/10.1016/S0040-1951(98)00160-7, 1998.

Fry, B., Deschamps, F., Kissling, E., Stehly, L., and Giardini, D.: Layered azimuthal anisotropy of Rayleigh wave phase velocities in the European Alpine lithosphere inferred from ambient noise, Earth Planet. Sci. Lett., 297, 95–102, https://doi.org/10.1016/j.epsl.2010.06.008, 2010.

Fuchs, W.: Gedanken zur Tektogenese der nördlichen Molasse zwischen Rhone und March, Jahrb. der Geol. Bundesanstalt, 119, 207–249, 1976.

Ganss, O. and Schmidt-Thomé, P.: Die gefaltete Molasse am Alpenrand zwischen Bodensee und Salzach, Zeitschrift der Dtsch. Geol. Gesellschaft, 105, 402–495, 1953.

Ganti, V., von Hagke, C., Scherler, D., Lamb, M. P., Fischer, W. W., and Avouac, J.-P.: Time scale bias in erosion rates of glaciated landscapes, Sci. Adv., 2, e1600204, https://doi.org/10.1126/sciadv.1600204, 2016.

Garefalakis, P. and Schlunegger, F.: Link between concentrations of sediment flux and deep crustal processes beneath the European Alps, Sci. Rep., 8, 183, https://doi.org/10.1038/s41598-017-17182-8, 2018.

Genser, J., Cloetingh, S., and Neubauer, F.: Late orogenic rebound and oblique Alpine convergence: New constraints from subsidence analysis of the Austrian Molasse basin, Global Planet. Change, 58, 214–223, https://doi.org/10.1016/j.gloplacha.2007.03.010, 2007.

Giamboni, M., Ustaszewski, K., Schmid, S. M., Schumacher, M. E., and Wetzel, A.: Plio-Pleistocene transpressional reactivation of Paleozoic and Paleogene structures in the Rhine-Bresse transform zone (northern Switzerland and eastern France), Int. J. Earth Sci., 93, 207–223, https://doi.org/10.1007/s00531-003-0375-2, 2004.

Glotzbach, C., Reinecker, J., Danišík, M., Rahn, M. K., Frisch, W., and Spiegel, C.: Thermal history of the central Gotthard and Aar massifs, European Alps: Evidence for steady state, long-term exhumation, J. Geophys. Res., 115, F03017, https://doi.org/10.1029/2009JF001304, 2010.

Glotzbach, C., van der Beek, P. A., and Spiegel, C.: Episodic exhumation and relief growth in the Mont Blanc massif, Western Alps from numerical modelling of thermochronology data, Earth Planet. Sci. Lett., 304, 417–430, https://doi.org/10.1016/j.epsl.2011.02.020, 2011.

Guellec, S., Mugnier, J.-L., Tardy, M., and Roure, F.: Neogene evolution of the western Alpine foreland in the light of ECORS data

and balanced cross-section, in: Deep structure of the Alps, Mém. Soc. géol. suisse, 1, edited by: Roure, F., Heitzmann, P., and Polino, R., Société Geologique Suisse, Zürich, 165–184, 1990.

Gusterhuber, J., Dunkl, I., Hinsch, R., Linzer, H.-G., and Sachsenhofer, R.: Neogene uplift and erosion in the Alpine Foreland Basin (Upper Austria and Salzburg), Geol. Carpathica, 63, 295–305, https://doi.org/10.2478/v10096-012-0023-5, 2012.

Haldemann, E. G., Haus, H. A., Holliger, A., Liechti, W., Rutsch, R. F., and della Valle, G.: Geological Atlas of Switzerland 1:25000, Map sheet Eggiwil (LK 1188), Federal Office of Topography swisstopo, Wabern, Switzerland, 1980.

Handy, M. R., Schmid, S. M., Bousquet, R., Kissling, E., and Bernoulli, D.: Reconciling plate-tectonic reconstructions of Alpine Tethys with the geological–geophysical record of spreading and subduction in the Alps, Earth-Science Rev., 102, 121–158, https://doi.org/10.1016/j.earscirev.2010.06.002, 2010.

Handy, M. R., Ustaszewski, K., and Kissling, E.: Reconstructing the Alps–Carpathians–Dinarides as a key to understanding switches in subduction polarity, slab gaps and surface motion, Int. J. Earth Sci., 104, 1–26, https://doi.org/10.1007/s00531-014-1060-3, 2015.

Haus, H.: Über alte Erosionserscheinungen am Südrand der miocaenen Nagelfluh des oberen Emmentales und deren Bedeutung für die Tektonik des Alpenrandes, Eclogae Geol. Helv., 28, 667–677, 1935.

Haus, H.: Geologie der Gegend von Schangnau im oberen Emmental (Kanton Bern): ein Beitrag zur Stratigraphie und Tektonik der subalpinen Molasse und des Alpenrandes, Beiträge zur Geol. Karte der Schweiz, Geologische Kommission der Schweizerischen Naturforschenden Gesellschaft, Bern, NF 75, 106 pp., 1937.

Herwegh, M., Berger, A., Baumberger, R., Wehrens, P., and Kissling, E.: Large-Scale Crustal-Block-Extrusion During Late Alpine Collision, Sci. Rep., 7, 413, https://doi.org/10.1038/s41598-017-00440-0, 2017.

Herwegh, M., Berger, A., Glotzbach, C., Wangenheim, C., Mock, S., Wehrens, P., Baumberger, R., Egli, D., and Kissling, E.: Late stages of continent-continent collision: Timing, kinematic evolution, and exhumation of the Northern rim (Aar Massif) of the Alps, Earth Sci. Rev., 200, 102959, https://doi.org/10.1016/j.earscirev.2019.102959, 2020.

Hetényi, G., Molinari, I., Clinton, J., Bokelmann, G., Bondár, I., Crawford, W. C., Dessa, J.-X., Doubre, C., Friederich, W., Fuchs, F., Giardini, D., Gráczer, Z., Handy, M. R., Herak, M., Jia, Y., Kissling, E., Kopp, H., Korn, M., Margheriti, L., Meier, T., Mucciarelli, M., Paul, A., Pesaresi, D., Piromallo, C., Plenefisch, T., Plomerová, J., Ritter, J., Rümpker, G., Šipka, V., Spallarossa, D., Thomas, C., Tilmann, F., Wassermann, J., Weber, M., Wéber, Z., Wesztergom, V., and Živčić, M.: The AlpArray Seismic Network: A Large-Scale European Experiment to Image the Alpine Orogen, Surv. Geophys., 39, 1009–1033, https://doi.org/10.1007/s10712-018-9472-4, 2018a.

Hetényi, G., Plomerová, J., Bianchi, I., Kampfová Exnerová, H., Bokelmann, G., Handy, M. R., and Babuška, V.: From mountain summits to roots: Crustal structure of the Eastern Alps and Bohemian Massif along longitude 13.3° E, Tectonophysics, 744, 239–255, https://doi.org/10.1016/j.tecto.2018.07.001, 2018b.

Hinsch, R.: Laterally varying structure and kinematics of the Molasse fold and thrust belt of the Central Eastern Alps: Implications for exploration, Am. Assoc. Pet. Geol. Bull., 97, 1805–1831, https://doi.org/10.1306/04081312129, 2013.

Homewood, P., Allen, P. A., and Williams, G. D.: Dynamics of the Molasse Basin of Western Switzerland, in: Foreland Basins, edited by: Allen, P. A. and Homewood, P., Blackwell Publishing Ltd., Oxford, UK, 199–217, https://doi.org/10.1002/9781444303810.ch10pp, 1986.

Hourigan, J. K., Reiners, P. W., and Brandon, M. T.: U-Th zonation-dependent alpha-ejection in (U-Th)/He chronometry, Geochim. Cosmochim. Ac., 69, 3349–3365, https://doi.org/10.1016/j.gca.2005.01.024, 2005.

Hurford, A. J.: Cooling and uplift patterns in the Lepontine Alps South Central Switzerland and an age of vertical movement on the Insubric fault line, Contrib. to Mineral. Petrol., 92, 413–427, 10.1007/BF00374424, 1986.

Jordi, H. A.: Blatt 1188 Eggiwil, Geol. Atlas Schweiz 1 25 000, Erläut. 75, Bundesamt für Landestopografie swisstopo, Wabern, 72 pp., ISBN 978-3-302-40065-5, 2012.

Karner, G. D. and Watts, A. B.: Gravity anomalies and flexure of the lithosphere at mountain ranges, J. Geophys. Res., 88, 10449–10477, https://doi.org/10.1029/JB088iB12p10449, 1983.

Kästle, E. D., Rosenberg, C., Boschi, L., Bellahsen, N., Meier, T., and El-Sharkawy, A.: Slab break-offs in the Alpine subduction zone, Int. J. Earth Sci., 109, 587–603, https://doi.org/10.1007/s00531-020-01821-z, 2020.

Kempf, O., Matter, A., Burbank, D. W., and Mange, M.: Depositional and structural evolution of a foreland basin margin in a magnetostratigraphic framework: the eastern Swiss Molasse Basin, Int. J. Earth Sci., 88, 253–275, https://doi.org/10.1007/s005310050263, 1999.

Ketcham, R. A.: Forward and Inverse Modeling of Low-Temperature Thermochronometry Data, Rev. Mineral. Geochemistry, 58, 275–314, https://doi.org/10.2138/rmg.2005.58.11, 2005.

Kissling, E. and Schlunegger, F.: Rollback Orogeny Model for the Evolution of the Swiss Alps, Tectonics, 37, 1097–1115, https://doi.org/10.1002/2017TC004762, 2018.

Kissling, E., Schmid, S. M., Lippitsch, R., Ansorge, J., and Fügenschuh, B.: Lithosphere structure and tectonic evolution of the Alpine arc: new evidence from high-resolution teleseismic tomography, Geol. Soc. London, Mem., 32, 129–145, https://doi.org/10.1144/GSL.MEM.2006.032.01.08, 2006.

Kuhlemann, J. and Kempf, O.: Post-Eocene evolution of the North Alpine Foreland Basin and its response to Alpine tectonics, Sediment. Geol., 152, 45–78, https://doi.org/10.1016/S0037-0738(01)00285-8, 2002.

Landesgeologie: Geological Map of Switzerland 1:500'000, Federal Office of Topography swisstopo, Wabern, Switzerland, 2005.

Landesgeologie: GeoMol: Geologisches 3D-Modell des Schweizer Molassebeckens – Schlussbericht, Bundesamt für Landestopografie swisstopo, Wabern, Berichte der Landesgeologie, 10, 128 pp., ISBN 978-3-302-40109-6, 2017.

Laubscher, H. P.: Die Fernschubhypothese der Jurafaltung, Eclogae Geol. Helv., 54, 221–280, 1961.

Laubscher, H. P.: Jura kinematics and the Molasse Basin, Eclogae Geol. Helv., 85, 653–675, 1992.

Leary, R., Orme, D. A., Laskowski, A. K., DeCelles, P. G., Kapp, P., Carrapa, B., and Dettinger, M.: Along-strike diachroneity in deposition of the Kailas Formation in central southern Tibet: Im-

plications for Indian slab dynamics, Geosphere, 12, 1198–1223, https://doi.org/10.1130/GES01325.1, 2016.

Lemcke, K.: Das Bayerische Alpenvorland vor der Eiszeit, Schweizerbart Science Publishers, Stuttgart, Germany, 1988.

Liniger, H.: Pliozän und Tektonik des Juragebirges, Eclogae Geol. Helv., 60, 407–490, 1967.

Lippitsch, R., Kissling, E., and Ansorge, J.: Upper mantle structure beneath the Alpine orogen from high-resolution teleseismic tomography, J. Geophys. Res., 108, 2376, https://doi.org/10.1029/2002JB002016, 2003.

Louis, S., Luijendijk, E., Dunkl, I., and Person, M.: Episodic fluid flow in an active fault, Geology, 47, 938–942, https://doi.org/10.1130/G46254.1, 2019.

Luijendijk, E.: Beo v1.0: numerical model of heat flow and low-temperature thermochronology in hydrothermal systems, Geosci. Model Dev., 12, 4061–4073, https://doi.org/10.5194/gmd-12-4061-2019, 2019.

Luijendijk, E., Winter, T., Köhler, S., Ferguson, G., von Hagke, C., and Scibek, J.: Using thermal springs to quantify deep groundwater flow and its thermal footprint in the Alps and North American orogens, EarthArXiv [preprint], https://doi.org/10.31223/osf.io/364dj, 29 April 2020.

Madritsch, H., Schmid, S. M., and Fabbri, O.: Interactions between thin- and thick-skinned tectonics at the northwestern front of the Jura fold-and-thrust belt (eastern France), Tectonics, 27, TC5005, https://doi.org/10.1029/2008TC002282, 2008.

Mair, D., Lechmann, A., Herwegh, M., Nibourel, L., and Schlunegger, F.: Linking Alpine deformation in the Aar Massif basement and its cover units – the case of the Jungfrau–Eiger mountains (Central Alps, Switzerland), Solid Earth, 9, 1099–1122, https://doi.org/10.5194/se-9-1099-2018, 2018.

Mazurek, M., Hurford, A. J., and Leu, W.: Unravelling the multi-stage burial history of the Swiss Molasse Basin: integration of apatite fission track, vitrinite reflectance and biomarker isomerisation analysis, Basin Res., 18, 27–50, https://doi.org/10.1111/j.1365-2117.2006.00286.x, 2006.

Mitterbauer, U., Behm, M., Brückl, E., Lippitsch, R., Guterch, A., Keller, G. R., Koslovskaya, E., Rumpfhuber, E.-M., and Šumanovac, F.: Shape and origin of the East-Alpine slab constrained by the ALPASS teleseismic model, Tectonophysics, 510, 195–206, https://doi.org/10.1016/j.tecto.2011.07.001, 2011.

Mock, S. and Herwegh, M.: Tectonics of the central Swiss Molasse Basin: Post-Miocene transition to incipient thick-skinned tectonics?, Tectonics, 36, 1699–1723, https://doi.org/10.1002/2017TC004584, 2017.

Molnar, P., England, P., and Martinod, J.: Mantle dynamics, uplift of the Tibetan Plateau, and the Indian Monsoon, Rev. Geophys., 31, 357–396, https://doi.org/10.1029/93RG02030, 1993.

Mosar, J.: Present-day and future tectonic underplating in the western Swiss Alps: reconciliation of basement/wrench-faulting and décollement folding of the Jura and Molasse basin in the Alpine foreland, Earth Planet. Sci. Lett., 173, 143–155, https://doi.org/10.1016/S0012-821X(99)00238-1, 1999.

Mosar, J., Stampfli, G. M., and François, G.: Western Préalpes Médianes Romandes: Timing and structure. A review, Eclogae Geol. Helv., 89, 389–425, 1996.

Mosbrugger, V., Utescher, T., and Dilcher, D. L.: Cenozoic continental climatic evolution of Central Europe, Proc. Natl. Acad. Sci., 102, 14964–14969, https://doi.org/10.1073/pnas.0505267102, 2005.

Müller, M., Nieberding, F., and Wanninger, A.: Tectonic style and pressure distribution at the northern margin of the Alps between Lake Constance and the River Inn, Geol. Rundschau, 77, 787–796, https://doi.org/10.1007/BF01830185, 1988.

Nussbaum, C.: Neogene tectonics and thermal maturity of sediments of the easternmost Southern Alps (Friuli area, Italy), PhD thesis, Université de Neuchâtel, 172 pp., 2000.

Oncken, O., Hindle, D., Kley, J., Elger, K., Victor, P., and Schemmann, K.: Deformation of the Central Andean Upper Plate System – Facts, Fiction, and Constraints for Plateau Models, in The Andes, in: Frontiers in Earth Sciences, edited by: Oncken, O., Chong, G., Franz, G., Giese, P., Götze, H.-J., Ramos, V. A., Strecker, M. R., and Wigger, P., Springer, Berlin, Heidelberg, Germany, 3–27, 2006.

Ortner, H., Reiter, F., and Brandner, R.: Kinematics of the Inntal shear zone–sub-Tauern ramp fault system and the interpretation of the TRANSALP seismic section, Eastern Alps, Austria, Tectonophysics, 414, 241–258, https://doi.org/10.1016/j.tecto.2005.10.017, 2006.

Ortner, H., Aichholzer, S., Zerlauth, M., Pilser, R., and Fügenschuh, B.: Geometry, amount, and sequence of thrusting in the Subalpine Molasse of western Austria and southern Germany, European Alps, Tectonics, 34, 1–30, https://doi.org/10.1002/2014TC003550, 2015.

Peresson, H. and Decker, K.: Far-field effects of Late Miocene subduction in the Eastern Carpathians: E-W compression and inversion of structures in the Alpine-Carpathian-Pannonian region, Tectonics, 16, 38–56, https://doi.org/10.1029/96TC02730, 1997.

Pfiffner, O. A.: Evolution of the North Alpine Foreland Basin in the Central Alps, in: Foreland Basins, edited by: Allen, P. A. and Homewood, P., Blackwell Publishing Ltd., Oxford, UK, 219–228, 1986.

Pfiffner, O. A.: Geologie der Alpen, 1st edn., Haupt, Bern, Stuttgart, Wien, 2009.

Pfiffner, O. A.: Structural Map of the Helvetic Zone of the Swiss Alps, including Vorarlberg (Austria) and Haute Savoie (France), 1 : 100 000, Federal Office of Topography swisstopo, Geol. Spec. Map, 128 (Explanatory notes), 2011.

Pfiffner, O. A., Erard, P. F., and Stäuble, M.: Two cross sections through the Swiss Molasse Basin (lines E4-E6, W1, W7-W10), in: Deep structure of the Swiss Alps. Results of NRP 20, edited by: Pfiffner, O. A., Lehner, P., Heitzmann, P., Mueller, S., and Steck, A., Birkhäuser, Basel, Boston, Berlin, 64–72, 1997.

Philippe, Y., Colletta, B., Deville, E., and Mascle, A.: The Jura fold-and-thrust belt: a kinematic model based on map-balancing, in: Peri Thetys Memoir 2: Structure and prospects of Alpine Basins and Forelands, edited by: Ziegler, P. A. and Horvàth, F., Muséum national d'Histoire naturelle, Paris, 235–261, 1996.

Pippèrr, M. and Reichenbacher, B.: Late Early Miocene palaeoenvironmental changes in the North Alpine Foreland Basin, Palaeogeogr. Palaeocl., 468, 485–502, https://doi.org/10.1016/j.palaeo.2017.01.002, 2017.

Qorbani, E., Bianchi, I., and Bokelmann, G.: Slab detachment under the Eastern Alps seen by seismic anisotropy, Earth Planet. Sci. Lett., 409, 96–108, https://doi.org/10.1016/j.epsl.2014.10.049, 2015.

Ratschbacher, L., Frisch, W., Linzer, H.-G., and Merle, O.: Lateral extrusion in the eastern Alps, PArt 2: Structural analysis, Tectonics, 10, 257–271, https://doi.org/10.1029/90TC02623, 1991.

Reiners, P. W. and Brandon, M. T.: Using Thermochronology to Understand Orogenic Erosion, Annu. Rev. Earth Planet. Sci., 34, 419–466, https://doi.org/10.1146/annurev.earth.34.031405.125202, 2006.

Rosenberg, C. L. and Berger, A.: On the causes and modes of exhumation and lateral growth of the Alps, Tectonics, 28, TC6001, https://doi.org/10.1029/2008TC002442, 2009.

Rosenberg, C. L. and Kissling, E.: Three-dimensional insight into Central-Alpine collision: Lower-plate or upper-plate indentation?, Geology, 41, 1219–1222, https://doi.org/10.1130/G34584.1, 2013.

Rosenberg, C. L., Berger, A., Bellahsen, N., and Bousquet, R.: Relating orogen width to shortening, erosion, and exhumation during Alpine collision, Tectonics, 34, 1306–1328, https://doi.org/10.1002/2014TC003736, 2015.

Rosenberg, C. L., Schneider, S., Scharf, A., Bertrand, A., Hammerschmidt, K., Rabaute, A., and Brun, J.-P.: Relating collisional kinematics to exhumation processes in the Eastern Alps, Earth-Sci. Rev., 176, 311–344, https://doi.org/10.1016/j.earscirev.2017.10.013, 2018.

Rutsch, R.: Molasse und Quartär im Gebiet des Siegfriedblattes Rüeggisberg (Kanton Bern), Beiträge zur Geol. Karte der Schweiz, Geologische Kommission der Schweizerischen Naturforschenden Gesellschaft, Bern, NF 87, 89 pp., 1947.

Sommaruga, A., Mosar, J., Schori, M., and Gruber, M.: The Role of the Triassic Evaporites Underneath the North Alpine Foreland, in Permo-Triassic Salt Provinces of Europe, North Africa and the Atlantic Margins, edited by: Soto, J. I., Flinch, J. F., and Tari, G., Elsevier, 447–466, 2017.

Schegg, R. and Leu, W.: Analysis of erosion events and palaeogeothermal gradients in the North Alpine Foreland Basin of Switzerland, Geol. Soc. London, Spec. Publ., 141, 137–155, https://doi.org/10.1144/GSL.SP.1998.141.01.09, 1998.

Schlunegger, F. and Castelltort, S.: Immediate and delayed signal of slab breakoff in Oligo/Miocene Molasse deposits from the European Alps, Sci. Rep., 6, 31010, https://doi.org/10.1038/srep31010, 2016.

Schlunegger, F. and Kissling, E.: Slab rollback orogeny in the Alps and evolution of the Swiss Molasse basin, Nat. Commun., 6, 8605, https://doi.org/10.1038/ncomms9605, 2015.

Schlunegger, F. and Mosar, J.: The last erosional stage of the Molasse Basin and the Alps, Int. J. Earth Sci., 100, 1147–1162, https://doi.org/10.1007/s00531-010-0607-1, 2011.

Schlunegger, F. and Norton, K. P.: Headward retreat of streams in the Late Oligocene to Early Miocene Swiss Alps, Sedimentology, 60, 85–101, https://doi.org/10.1111/sed.12010, 2013.

Schlunegger, F. and Norton, K. P.: Climate vs. tectonics: the competing roles of Late Oligocene warming and Alpine orogenesis in constructing alluvial megafan sequences in the North Alpine foreland basin, Basin Res., 27, 230–245, https://doi.org/10.1111/bre.12070, 2015.

Schlunegger, F., Matter, A., and Mange, M. A.: Alluvial fan sedimentation and structure of the southern Molasse Basin margin, Lake Thun area, Switzerland, Eclogae Geol. Helv., 86, 717–750, 1993.

Schlunegger, F., Burbank, D. W., Matter, A., Engesser, B., and Mödden, C.: Magnetostratigraphic calibration of the Oligocence to Middle Miocene (30-15 Ma) mammal biozones and depositional sequences of the Swiss Molasse Basin, Eclogae Geol. Helv., 89, 753–788, 1996.

Schlunegger, F., Matter, A., Burbank, D. W., and Klaper, E. M.: Magnetostratigraphic constraints on relationships between evolution of the central Swiss Molasse basin and Alpine orogenic events, Geol. Soc. Am. Bull., 109, 225–241, https://doi.org/10.1130/0016-7606(1997)109<0225:MCORBE>2.3.CO;2, 1997.

Schlunegger, F., Rieke-Zapp, D., and Ramseyer, K.: Possible environmental effects on the evolution of the Alps-Molasse Basin system, Swiss J. Geosci., 100, 383–405, https://doi.org/10.1007/s00015-007-1238-9, 2007.

Schlunegger, F., Anspach, O., Bieri, B., Böning, P., Kaufmann, Y., Lahl, K., Lonschinski, M., Mollet, H., Sachse, D., Schubert, C., Stöckli, G., and Zander, I.: Geological Atlas of Switzerland 1:25000, Map sheet Schüpfheim (LK 1169), Federal Office of Topography swisstopo, Wabern, Switzerland, 2016.

Schmid, S. M., Pfiffner, O. A., Froitzheim, N., Schönborn, G., and Kissling, E.: Geophysical-geological transect and tectonic evolution of the Swiss-Italian Alps, Tectonics, 15, 1036–1064, https://doi.org/10.1029/96TC00433, 1996.

Schmid, S. M., Fügenschuh, B., Kissling, E., and Schuster, R.: Tectonic map and overall architecture of the Alpine orogen, Eclogae Geol. Helv., 97, 93–117, https://doi.org/10.1007/s00015-004-1113-x, 2004.

Schmid, S. M., Scharf, A., Handy, M. R., and Rosenberg, C. L.: The Tauern Window (Eastern Alps, Austria): a new tectonic map, with cross-sections and a tectonometamorphic synthesis, Swiss J. Geosci., 106, 1–32, https://doi.org/10.1007/s00015-013-0123-y, 2013.

Schmid, S. M., Kissling, E., Diehl, T., van Hinsbergen, D. J. J., and Molli, G.: Ivrea mantle wedge, arc of the Western Alps, and kinematic evolution of the Alps–Apennines orogenic system, Swiss J. Geosci., 110, 581–612, https://doi.org/10.1007/s00015-016-0237-0, 2017.

Schönborn, G.: Alpine tectonics and kinematic models of the central Southern Alps, Mem. di Sci. Geol. Padova, 44, 229–393, 1992.

Schuller, V., Frisch, W., and Herzog, U.: Critical taper behaviour and out-of-sequence thrusting on orogenic wedges – an example of the Eastern Alpine Molasse Basin, Terra Nov., 27, 231–237, https://doi.org/10.1111/ter.12152, 2015.

Sinclair, H. D.: Flysch to molasse transition in peripheral foreland basins: The role of the passive margin versus slab breakoff, Geology, 25, 1123–1126, https://doi.org/10.1130/0091-7613(1997)025<1123:FTMTIP>2.3.CO;2, 1997.

Sinclair, H. D. and Allen, P. A.: Vertical versus horizontal motions in the Alpine orogenic wedge: stratigraphic response in the foreland basin, Basin Res., 4, 215–232, https://doi.org/10.1111/j.1365-2117.1992.tb00046.x, 1992.

Sinclair, H. D., Coakley, B. J., Allen, P. A., and Watts, A. B.: Simulation of Foreland Basin Stratigraphy using a diffusion model of mountain belt uplift and erosion: An example from the central Alps, Switzerland, Tectonics, 10, 599–620, https://doi.org/10.1029/90TC02507, 1991.

Sommaruga, A.: Décollement tectonics in the Jura forelandfold-and-thrust belt, Mar. Petrol. Geol., 16, 111–134, https://doi.org/10.1016/S0264-8172(98)00068-3, 1999.

Sommaruga, A., Eichenberger, U., and Marillier, F.: Seismic Atlas of the Swiss Molasse Basin, Matériaux pour la Géologie la Suisse - Géophysique, 44, Swiss Geophysical Commission, Federal Office of Topography swisstopo, Wabern, ISBN 978-3-302-40064-82012, 2012.

Spiegel, C., Kuhlemann, J., Dunkl, I., and Frisch, W.: Paleogeography and catchment evolution in a mobile orogenic belt: the Central Alps in Oligo–Miocene times, Tectonophysics, 341, 33–47, https://doi.org/10.1016/S0040-1951(01)00187-1, 2001.

Stampfli, G. M. and Marchant, R. H.: Geodynamic evolution of the Tethyan margins of the Western Alps, in: Deep structure of the Swiss Alps: Results of NRP 20, edited by: Pfiffner, O. A., Lehner, P., Heitzmann, P., Mueller, S., and Steck, A., Birkhäuser, Basel, Boston, Berlin, 223–240, 1997.

Stäuble, M. and Pfiffner, O. A.: Processing, interpretation and modeling of seismic reflection data in the Molasse Basin of eastern Switzerland, Eclogae Geol. Helv., 84, 151–175, https://doi.org/10.5169/seals-166767, 1991.

Strunck, P. and Matter, A.: Depositional evolution of the western Swiss Molasse, Eclogae Geol. Helv., 95, 197–222, https://doi.org/10.5169/seals-168955, 2002.

Ustaszewski, K. and Schmid, S. M.: Latest Pliocene to recent thick-skinned tectonics at the Upper Rhine Graben – Jura Mountains junction, Swiss J. Geosci., 100, 293–312, https://doi.org/10.1007/s00015-007-1226-0, 2007.

Ustaszewski, K., Schmid, S. M., Fügenschuh, B., Tischler, M., Kissling, E., and Spakman, W.: A map-view restoration of the Alpine-Carpathian-Dinaridic system for the Early Miocene, Swiss J. Geosci., 101, 273–294, https://doi.org/10.1007/s00015-008-1288-7, 2008.

Valla, P. G., van der Beek, P. A., Shuster, D. L., Braun, J., Herman, F., Tassan-Got, L., and Gautheron, C.: Late Neogene exhumation and relief development of the Aar and Aiguilles Rouges massifs (Swiss Alps) from low-temperature thermochronology modeling and ^{4}He/^{3}He thermochronometry, J. Geophys. Res., 117, F01004, https://doi.org/10.1029/2011JF002043, 2012.

Vermeesch, P.: Three new ways to calculate average (U–Th)/He ages, Chem. Geol., 249, 339–347, https://doi.org/10.1016/j.chemgeo.2008.01.027, 2008.

Vernon, A. J., van der Beek, P. A., Sinclair, H. D., Persano, C., Foeken, J., and Stuart, F. M.: Variable late Neogene exhumation of the central European Alps: Low-temperature thermochronology from the Aar Massif, Switzerland, and the Lepontine Dome, Italy, Tectonics, 28, TC5004, https://doi.org/10.1029/2008TC002387, 2009.

Vollmayr, T.: Strukturelle Ergebnisse der Kohlenwasserstoffexploration im Gebiet von Thun, Schweiz, Eclogae Geol. Helv., 85, 531–539, 1992.

von Hagke, C. and Malz, A.: Triangle zones – Geometry, kinematics, mechanics, and the need for appreciation of uncertainties, Earth-Sci. Rev., 177, 24–42, https://doi.org/10.1016/j.earscirev.2017.11.003, 2018.

von Hagke, C., Cederbom, C. E., Oncken, O., Stöckli, D. F., Rahn, M. K., and Schlunegger, F.: Linking the northern Alps with their foreland: The latest exhumation history resolved by low-temperature thermochronology, Tectonics, 31, TC5010, https://doi.org/10.1029/2011TC003078, 2012.

von Hagke, C., Oncken, O., and Evseev, S.: Critical taper analysis reveals lithological control of variations in detachment strength: An analysis of the Alpine basal detachment (Swiss Alps), Geochem., Geophy. Geosy., 15, 176–191, https://doi.org/10.1002/2013GC005018, 2014a.

von Hagke, C., Oncken, O., Ortner, H., Cederbom, C. E., and Aichholzer, S.: Late Miocene to present deformation and erosion of the Central Alps – Evidence for steady state mountain building from thermokinematic data, Tectonophysics, 632, 250–260, https://doi.org/10.1016/j.tecto.2014.06.021, 2014b.

Wehrens, P., Baumberger, R., Berger, A., and Herwegh, M.: How is strain localized in a meta-granitoid, mid-crustal basement section? Spatial distribution of deformation in the central Aar massif (Switzerland), J. Struct. Geol., 94, 47–67, https://doi.org/10.1016/j.jsg.2016.11.004, 2017.

Weidmann, M., Homewood, P., Morel, R., Berchten, J.-D., Bucher, H., Burri, M., Cornioley, J.-D., Escher, P., Rück, P., Tabotta, A., and Zahner, P.: Geological Atlas of Switzerland 1 : 25 000, Map sheet Châtel-St-Denis (LK 1244), Federal Office of Topography swisstopo, Wabern, Switzerland, 1993.

Weisenberger, T. B., Rahn, M. K., van der Lelij, R., Spikings, R. A., and Bucher, K.: Timing of low-temperature mineral formation during exhumation and cooling in the Central Alps, Switzerland, Earth Planet. Sci. Lett., 327–328, 1–8, https://doi.org/10.1016/j.epsl.2012.01.007, 2012.

Whipple, K. X.: The influence of climate on the tectonic evolution of mountain belts, Nat. Geosci., 2, 97–104, https://doi.org/10.1038/ngeo413, 2009.

Willett, S. D. and Schlunegger, F.: The last phase of deposition in the Swiss Molasse Basin: from foredeep to negative-alpha basin, Basin Res., 22, 623–639, https://doi.org/10.1111/j.1365-2117.2009.00435.x, 2010.

Willett, S. D., Schlunegger, F., and Picotti, V.: Messinian climate change and erosional destruction of the central European Alps, Geology, 34, 613–616, https://doi.org/10.1130/G22280.1, 2006.

Wolf, R. A., Farley, K. A., and Silver, L. T.: Helium diffusion and low-temperature thermochronometry of apatite, Geochim. Cosmochim. Ac., 60, 4231–4240, https://doi.org/10.1016/S0016-7037(96)00192-5, 1996.

Zaugg, A., Löpfe, R., Kriemler, M., and Kempf, T.: Geological Atlas of Switzerland 1 : 25 000, Federal Office of Topography swisstopo, Wabern, Switzerland, 2011.

Zhao, L., Paul, A., Malusà, M. G., Xu, X., Zheng, T., Solarino, S., Guillot, S., Schwartz, S., Dumont, T., Salimbeni, S., Aubert, C., Pondrelli, S., Wang, Q., and Zhu, R.: Continuity of the Alpine slab unraveled by high-resolution P wave tomography, J. Geophys. Res.-Sol. Ea., 121, 8720–8737, https://doi.org/10.1002/2016JB013310, 2016.

Zweigel, J., Aigner, T., and Luterbacher, H.: Eustatic versus tectonic controls on Alpine foreland basin fill: sequence stratigraphy and subsidence analysis in the SE German Molasse, in Cenozoic Foreland basins of Western Europe, edited by: Mascle, A., Puigdefàbregas, C., Luterbacher, H. P., and Fernàndez, M., Geological Society Special Publications, 134, 299–323, https://doi.org/10.1144/GSL.SP.1998.134.01.14, 1998.